國立臺灣大學生命科學院植物科學研究所

碩士論文

Institute of Plant Biology
College of Life Science
National Taiwan University
Master's Thesis

阿拉伯芥組蛋白去乙醯基酶 HDA5 在熱逆境中之功能性研究

Functional study of histone deacetylase HDA5 in response to thermal stress in Arabidopsis

王胤棨

Yin-Chi Wang

指導教授：靳宗洛 博士

Advisor: Tsung-Luo Jinn, Ph.D

中華民國 114 年 1 月

January, 2025

doi:10.6342/NTU202500611

致謝

在植科所兩年半的時間，能夠完成這篇論文，首先要感謝靳宗洛老師，感謝您提供了完善的環境和資源能讓我安心做實驗。謝謝剛進來的時候遇到的宇豪學長、Sandeep 以及 Silambu 幫助我快速進入狀況及實驗上的指導，也謝謝品萱、芷淇、瑞德和顗安平常的的打屁聊天、實驗上的討論以及工作上的幫助。Silambu, I wish you success in publishing your paper and finding a great job. Sandeep, thank you for your help over the past two and a half years—I hope you graduate soon and enjoy a wonderful marriage. Wishing you both all the best! 也祝福千又跟芝穎接下來的實驗以及在台大的時光能開心順利。另外也要謝謝施元心學姐的幫助，從實驗設計、器材借用到數據分析都不留餘力的幫忙我。

最後我要感謝我自己，碩二下開始的很多事情都變了調，生離死別都體驗了一輪，感謝自己能夠撐下來，接下來也加油，照著想像的畫面去活。

胤棨 2025.02.10

doi:10.6342/NTU202500611

摘要

先前研究已經闡明部分與植物熱逆境反應相關的轉錄調控網絡，然而關於轉錄靜默和染色質重塑的機制仍然未知。組蛋白去乙醯基酶 (HDACs) 是與轉錄靜默緊密相連的關鍵染色質調控因子，對植物適應不良環境至關重要。阿拉伯芥微陣列分析顯示，熱逆境誘導 *HDA5* 的表達，但其功能與機制仍然不明。在本研究中透過兩種熱耐性測試：基礎耐熱性及後天耐熱性確認 HDA5 在熱逆境反應途徑中作為負調控因子。進一步透過蛋白交互作用實驗發現，在 19 個熱休克因子（HSFs）中，HDA5 會與 HSFA1d，HSFA8，HSFA9 以及 HSFB2b 在細胞核中有相互作用。qPCR 分析表明，在 *hda5-1* 突變株中，與野生型相比，多個 *HSFs* 的表達量增加，並且其下游基因 *HSP22* 與 *HSP101* 的表現量顯著增加。ChIP-qPCR 分析發現，在 *hda5-1* 突變體中，*HSP22* 啟動子的 H3K9 乙醯化的程度顯著提升，而在 *HSP101* 啟動子則未出現變化。此外，*HSP22* 啟動子上的 H3K9 乙醯化與 H3K4 二甲基化的豐度之間存在拮抗關係，且 *HSP101* 啟動子的 H3K4 二甲基化的程度呈下降趨勢。在原生質體次細胞定位實驗中中發現 HDA5 在正常生長環境下出現在細胞核中，在熱逆境的環境下則是完全轉移至細胞核外，這表明 HDA5 可能間接調控熱相關基因 （heat-responsive genes）。Dual-luciferase reporter 實驗顯示，HDA5 與 HSFB2b 共同作用，顯著抑制了 *HSP22* 的轉錄活性。根據上述研究結果推測，HDA5 在熱反應中可能透過非組蛋白為目標的蛋白質去乙醯化（deacetylation）與調控組蛋白修飾相關蛋白來實現對轉錄組的轉錄沉默，而非直接參與組蛋白修飾（histone modification）。

doi:10.6342/NTU202500611

Key Words: 阿拉伯芥，表觀遺傳，去乙醯基蛋白，去乙醯基化，甲基化，非生物逆境，耐熱性，熱休克轉錄因子，熱休克蛋白

doi:10.6342/NTU202500611

Abstract

Research has highlighted the complex regulatory networks involved in plant heat shock responses (HSR), yet the mechanisms underlying chromatin remodeling and transcriptional silencing during HS adaptation remain elusive. Histone deacetylases (HDACs) are key chromatin regulators linked to transcriptional silencing, essential for plant resilience in adverse environments. Arabidopsis microarray data indicates that heat stress induces *HDA5*, but its precise role remains unclear. This study reveals that HDA5 functions as a negative regulator in the heat stress response and that thermotolerance tests confirm its regulatory role under both baseline and acquired heat stress conditions. Further analysis of protein-protein interactions data showed that among 19 heat shock factors (HSFs), HDA5 interacts with HSFA1d, HSFA8, HSFA9, and HSFB2b in the nucleus. qPCR analysis revealed that in the *hda5-1* mutant, several *HSFs* were upregulated compared to the wild type (Col-0), with downstream genes *HSP22* and *HSP101* showing significant increases in expression. ChIP-qPCR analysis revealed an increase in H3K9 acetylation at the *HSP22* loci in the *hda5-1* mutant, while no changes were observed at the *HSP101* loci. Additionally, an antagonistic relationship between H3K9 acetylation and H3K4 dimethylation was observed at the *HSP22* loci, accompanied by a downtrend in H3K4 dimethylation at the *HSP101* loci. Subcellular localization

doi:10.6342/NTU202500611

studies showed that HDA5 relocates from the nucleus to the cytoplasm under HS, suggesting that HDA5 may regulate heat-responsive genes indirectly. Dual-luciferase reporter assays revealed that HDA5, in conjunction with HSFB2b, significantly inhibits the transcriptional activity of *HSP22*. These findings propose a novel role for HDA5 in transcriptional silencing during HS, potentially through the deacetylation of non-histone proteins or modulation of histone modification-related proteins, rather than direct histone modification.

Key Words: Arabidopsis, epigenetic, histone deacetylase, deacetylation, methylation, abiotic stress, thermotolerance, heat shock factor, heat shock protein

doi:10.6342/NTU202500611

Table of contents

doi:10.6342/NTU202500611

doi:10.6342/NTU202500611

List of figures

doi:10.6342/NTU202500611

doi:10.6342/NTU202500611

List of tables

doi:10.6342/NTU202500611

Abbreviations

AT	Acquired Thermotolerance
BT	Basal Thermotolerance
CDS	Coding Sequence
ChIP	Chromatin Immunoprecipitation
DBD	DNA Binding Domain
ER	Endoplasmic Reticulum
HAT	Histone Acetyltransferase
HDAC	Histone Deacetylase
HDM	Histone Methyltransferase
HMT	Histone Demethylase
HS	Heat Stress
HSF	Heat Shock Factor
HSP	Heat Shock Protein
HSR	Heat Shock Response
KO	Knockout
LAT	Long-term Acquired Thermotolerance
PTM	Post Translational Modification

doi:10.6342/NTU202500611

OD	Oligomerization Domain
OE	Overexpression
RbcL	Rubisco Large subunit
ROS	Reactive Oxygen Species
SAT	Short-term Acquired Thermotolerance
UPR	Unfold Protein Response

doi:10.6342/NTU202500611

Introduction

Climate change is expected to intensify the frequency of extreme natural disasters, which will significantly reduce crop yields. Events such as high temperatures, severe floods, and prolonged droughts can have devastating effects on plant survival. Unlike mobile organisms, plants are unable to escape harmful conditions by relocating to safer environments. Instead, they have developed a variety of molecular mechanisms to detect and respond to diverse environmental stresses, including heat, salinity, drought, and oxidative stress (Demidchik, 2015; Fang and Xiong, 2015; Ohama et al., 2017). Despite extensive research efforts aimed at understanding how plants adapt to abiotic stresses, many aspects of these mechanisms remain poorly understood and warrant further investigation.

Heat Shock Response (HSR) and Thermotolerance

Heat shock response (HSR) is a protective mechanism that triggers the transcription and translation of proteins or enzymes to prevent the damage caused by heat stress (HS) (Wahid et al., 2007). This evolutionarily conserved process is observed in both prokaryotic and eukaryotic organisms. In plants, HS typically refers to an increase in ambient temperature of 10–15°C above optimal levels (Wahid et al., 2007). Such

doi:10.6342/NTU202500611

conditions induce protein misfolding, reduce enzyme activity, and trigger the accumulation of reactive oxygen species (ROS) and impairing plant functions. These effects ultimately disrupt normal physiological processes.

As immobile organisms, plants possess basal thermotolerance (BT), enabling them to endure high temperatures without prior exposure. In contrast, acquired thermotolerance (AT) allows plants to survive lethal heat stress following brief acclimation at moderately high temperatures (Vierling, 1991; Larkindale et al., 2005). At the molecular level, these thermotolerances are linked to the HSR.

The initiation of the HSR in plants begins with thermosensing. Recent studies suggest that DNA, RNA, proteins, and membrane fluidity act as thermosensors (Mittler et al., 2012; Vu et al., 2019). At lower temperatures, the histone variant H2A.Z is highly abundant in nucleosomes and occupies DNA regions, hindering transcription by preventing RNA Polymerase II from binding to the cis-elements of target genes. As a result, H2A.Z acts as a physical barrier that represses gene expression at low temperatures. When temperatures rise, the occupancy of H2A.Z nucleosomes decreases, leading to the upregulation of genes such as *HSP70* (Kumar and Wigge, 2010; Cortijo et al., 2017). Furthermore, the deposition of H2A.Z is regulated by POWERDRESS (PWR) and

doi:10.6342/NTU202500611

HISTONE DEACETYLASE 9 (HDA9) under high-temperature conditions, which are critical for HSR (Tasset et al., 2018). In summary, temperature-induced chromatin remodeling modulates transcriptional activity and serves as a thermosensor to trigger downstream signaling pathways in response to temperature fluctuations.

Heat stress also induces the accumulation of misfolded proteins in the endoplasmic reticulum (ER), causing ER stress and activating the unfolded protein response (UPR) in plants (Manghwar and Li, 2022). The ER is a vital cytoplasmic membrane system in eukaryotic cells, involved in protein synthesis, peptide chain folding, post-translational modifications, lipid biosynthesis, and calcium storage and homeostasis. ER stress disrupts ER homeostasis, impairing plant physiological functions.

The UPR is regulated by intramembrane proteolysis of basic leucine zipper (bZIP) transcription factors such as bZIP17, bZIP28, and bZIP60 (Nawkar et al., 2018). One pathway involves bZIP17 and bZIP28. Under normal conditions, these transcription factors are anchored to the ER membrane by their interaction with binding protein (BiP). During HS, the accumulation of misfolded proteins activates BiP, which aids in proper protein folding and releases bZIP17 and bZIP28 from the ER membrane. These transcription factors are then transported to the Golgi via COAT PROTEIN II (COPII)

doi:10.6342/NTU202500611

vesicles, where SITE-1 and -2 proteases process them. This processing releases bZIP17 and bZIP28, enabling their translocation into the nucleus, where they form transcriptional complexes to activate UPR-related genes.

Another UPR pathway is mediated by bZIP60 and the RNase INOSITOL-REQUIRING ENZYME 1 (IRE1) (Howell, 2021). Although the detailed mechanism of this pathway requires further investigation, it is known that IRE1 splices bZIP60, enabling its translocation into the nucleus, where it mediates the UPR.

In conclusion, the diversity of HSR mechanisms in plants equips them to withstand severe HS conditions. These processes reduce damage from HS and maintain homeostasis, ensuring survival under stressful environmental conditions.

Heat Shock Factors (HSFs) and Transcriptional Regulation

Heat shock factors (HSFs) are essential transcriptional regulators that orchestrate the HSR in plants by activating the expression of heat shock proteins (HSPs) and other stress-responsive genes. In Arabidopsis, HSFs constitute a large multigene family, with 21 members classified into three major groups: HSFA, HSFB, and HSFC, based on their structural features and functional domains (Nover et al., 2001). HSFs typically feature four conserved regions: a DNA-binding domain (DBD), oligomerization domain

doi:10.6342/NTU202500611

(OD/HR-A/B), nuclear localization/export signals (NLS/NES), and activator motifs (AHA motifs) (Wu, 1995; Nover et al., 2001). The DBD, located at the N-terminus, recognizes and binds heat shock elements (HSEs) in the promoters of stress-response genes. The OD facilitates HSF trimerization, with class A HSFs having 21 amino acid insertions, class C having 7, and class B possessing flexible linkers in the HR-A/B region. The NLS and NES control nuclear transport, while the C-terminal AHA motif in class A HSFs enables transcriptional activation. In contrast, class B HSFs carry a repression domain, functioning as transcriptional repressors (von Koskull-Döring et al., 2007).

Among Arabidopsis HSFs, HSFA1a, HSFA1b, and HSFA1d are considered master regulators of the HSR, acting upstream to regulate the expression of downstream *HSFs* and *HSPs* (Lohmann et al., 2004). The quadruple knockout (QK) mutant of *hsfa1s* shows severe defects in both basal and acquired thermotolerance, along with drastically reduced expression of key HS-related genes such as *DREB2A*, *HSFA2*, *HSFA3*, *HSFA7a*, and *HSFA7b*, leading to heat sensitivity (Liu et al., 2011; Liu and Charng, 2013).

HSFA2 is a highly inducible HSF during heat stress, critical for HS transcriptional memory and the activation of downstream genes regulating HSR (Charng et al., 2007; Schramm et al., 2006). *HSFA3*, uniquely induced by DREB2A, supports heat shock

doi:10.6342/NTU202500611

protein (HSP) expression and enhances thermotolerance (Yoshida et al., 2008). Recent studies show that HSFA2 and HSFA3 can form heterotrimers to regulate HS transcriptional memory and maintain the expression of memory-related genes (Friedrich et al., 2021).

HSFA7a and *HSFA7b* are strongly induced by heat stress (Liu et al., 2011). *HSFA7a* is also upregulated by azetidine-2-carboxylic acid (AZC), a treatment that triggers the cytosolic protein response by accumulating misfolded proteins, highlighting its complex role in heat stress responses (Lin et al., 2018). *HSFA7b* acts as a positive regulator, binding to E-box motifs and contributing to salinity tolerance (Zang et al., 2019).

HSFA8 has been shown to function as a redox sensor in plants, with its conserved cysteinyl residues detecting oxidative changes. In response to H_2O_2 treatment, HSFA8 translocates from the cytosol to the nucleus to regulate the oxidative stress response (Giesguth et al., 2015; Andrási et al., 2020). Meanwhile, HSFA9 plays a crucial role in seed longevity by activating the expression of specialized HSPs during the late stages (Kotak et al., 2007; Tejedor-Cano et al., 2010).

HSFB2b belongs to the class B HSFs and functions primarily as a transcriptional repressor. Studies have shown that HSFB2b, along with HSFB1, suppresses the

doi:10.6342/NTU202500611

expression of heat-inducible HSFs, such as *HSFA2* and *HSFA7a*, under non-stress conditions. This repression maintains basal levels of HSPs when plants are not exposed to heat stress (Ikeda et al., 2011).

In the same study that authors revealed HSFB2b also plays a positive role in acquired thermotolerance. During heat stress, HSFB2b is required for the expression of specific HSP genes, contributing to the plant's ability to withstand elevated temperatures. This dual function highlights the complex regulatory role of HSFB2b in balancing heat-responsive gene expression under normal and stress conditions.

Additionally, HSFB2b interacts with other transcription factors, influencing diverse stress-response pathways. For example, it mediates the repression of *PRR7*, a regulator of the circadian clock, thereby integrating abiotic stress responses with circadian rhythms (Huang et al., 2015).

Beyond abiotic stress responses, HSFB2b is involved in regulating biotic stress responses (Pick et al., 2012). T-DNA knockout mutants of *hsfb2b* and double knockout mutant *hsfb1/b2b*, revealed that these transcription factors negatively regulate the basal expression of defensin genes *pdf1.2a/b*, which are critical for defense against necrotrophic pathogens. Interestingly, the expression of *pdf1.2* was strongly upregulated,

doi:10.6342/NTU202500611

even under basal conditions, and further enhanced upon jasmonic acid treatment or infection with *Alternaria brassicicola*.

Heat Shock Proteins (HSPs)

Heat shock proteins (HSPs) are a group of highly conserved molecular chaperones that play a crucial role in protecting plants against stress-induced damage, particularly during heat stress (HS). In Arabidopsis, HSPs are rapidly upregulated in response to elevated temperatures, aiding in the proper folding of nascent polypeptides, refolding of misfolded proteins, and preventing protein aggregation (Vierling, 1991). HSPs are classified into several families based on their molecular weight, including HSP100, HSP90, HSP70, HSP60, and small HSPs (sHSPs), each with distinct functions in cellular homeostasis (Kotak et al., 2007).

Among these, HSP70 and HSP101 are particularly critical in acquired thermotolerance (AT), where plants develop tolerance to lethal temperatures after brief exposure to sub-lethal heat (Kotak et al., 2007). HSP101, a member of the ClpB family, is indispensable for disaggregating stress-damaged proteins, a process that requires cooperation with HSP70 (Queitsch et al., 2000).

doi:10.6342/NTU202500611

Small HSPs (sHSPs), such as HSP18.2 and HSP22, play pivotal roles in cellular protection during HS. HSP18.2 is a cytosolic sHSP that forms large oligomers to sequester misfolded proteins, preventing their aggregation and subsequent toxicity (Scharf et al., 2001). HSP18.2 is one of the most abundantly expressed sHSPs during HS and is commonly used as a marker for heat stress studies. On the other hand, HSP22, a mitochondrial-localized sHSP, prevents protein aggregation and protects mitochondrial integrity under heat stress (Heckathorn et al., 1999; Sun et al., 2002). Its expression is tightly regulated by heat shock factors (HSFs) and correlates with enhanced thermotolerance. Both HSP18.2 and HSP22 are indispensable for maintaining cellular homeostasis under stress and are integral to the heat stress response (HSR).

The transcription of *HSP* genes is regulated by heat shock factors (HSFs), with HSFA1s acting as master regulators of the HSR (Yoshida et al., 2011). During HS, HSFs bind to conserved HSEs in the promoters of *HSP* genes, triggering their expression. Furthermore, chromatin remodeling processes, including histone acetylation, have been implicated in modulating *HSP* expression, suggesting a complex regulatory network underlying HSR (Tasset et al., 2018).

doi:10.6342/NTU202500611

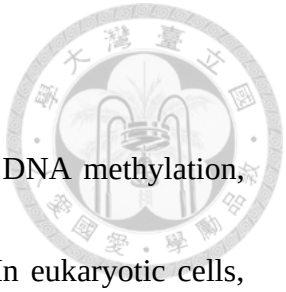

Histone Acetylation and Methylation

Epigenetic modifications, including histone modifications and DNA methylation, are heritable markers that regulate gene expression in eukaryotes. In eukaryotic cells, genomic DNA is packaged into chromosomes within the nucleus. Chromosomes are primarily composed of histone proteins, which form nucleosomes by wrapping genomic DNA around them. A nucleosome consists of an octamer of histones—two copies each of H2A, H2B, H3, and H4—around which 145–147 base pairs of DNA are wound in 1.65 left-handed turns (Luger et al., 1997).

Each histone protein includes a structured globular domain and an unstructured N-terminal tail, which is subject to post-translational modifications (PTMs) such as methylation, acetylation, phosphorylation, ubiquitination, glycosylation, ADP-ribosylation, and sumoylation (Bannister and Kouzarides, 2011). These modifications alter chromatin structure, impacting transcription, DNA repair, replication, and recombination (Berger, 2007; Klose and Yi, 2007).

Histone acetylation occurs primarily on lysine residues of histones H3 and H4 and is dynamically regulated by histone acetyltransferases (HATs) and histone deacetylases (HDACs). HATs add acetyl groups to lysines, loosening chromatin structure and promoting transcriptional activation. Conversely, HDACs remove acetyl groups, leading

doi:10.6342/NTU202500611

to chromatin condensation and transcriptional repression (Berger, 2007; Klose and Yi, 2007).

In *Arabidopsis thaliana*, HDACs have diverse roles in plant development and stress responses. For example, HDA6, a class I RPD3/HDA1-type HDAC, regulates embryo development, flowering time, and jasmonic acid response (Liu et al., 2016). HDA6 also interacts with histone demethylases, such as FLOWERING LOCUS D (FLD) and LDL1/2, to control flowering and circadian rhythms (Yu et al., 2011). Additionally, HDA6 partners with ASYMMETRIC LEAVES 1/2 (AS1/2) to repress *KNOTTED-LIKE HOMOBOX (KNOX)* gene expression, influencing leaf development (Luo et al., 2012).

Histone methylation, which occurs on lysine and arginine residues, is another critical modification for transcription regulation (Berger, 2007; Klose and Yi, 2007). This process is mediated by histone methyltransferases (HMTs) and histone demethylases (HDMs). Lysines 4, 9, 27, and 36 of histone H3, and lysine 20 of histone H4, are common methylation sites catalyzed by histone lysine methyltransferases (HKMTs).

The functional outcome of methylation depends on the site and type of methylation. For instance, H3K9me and H3K27me are associated with transcriptional repression, while H3K4me and H3K36me are linked to transcriptional activation (Berger, 2007;

doi:10.6342/NTU202500611

Klose and Yi, 2007). HKMTs can transfer one, two, or three methyl groups to lysines, with varying effects on gene expression. For example, H3K9 monomethylation (H3K9me1) and dimethylation (H3K9me2) suppress transposon activity, with H3K9me2 enriched in transposons and repetitive sequences (Bernatavichute et al., 2008; Liu et al., 2010; Stroud et al., 2014; Du et al., 2015). In contrast, H3K9 trimethylation (H3K9me3) is enriched in euchromatin, where most active genes reside (Liu et al., 2010).

Histone Deacetylases (HDACs)

In eukaryotes, transcriptional regulation is closely linked to chromatin structure, which is significantly influenced by histone posttranslational modifications such as acetylation, methylation, phosphorylation, and ubiquitination (Berger, 2002). Histone acetylation, a reversible process, is regulated by histone acetyltransferases (HATs) and histone deacetylases (HDACs), with HDACs removing acetyl groups from ε-N-acetyl lysine residues (Hollender and Liu, 2008; Liu et al., 2014).

Mammalian HDACs are categorized into four classes based on phylogenetic and structural similarities (Gregoretti et al., 2004). Zinc-dependent HDACs include class I (HDAC1, HDAC2, HDAC3, HDAC8), class IIa (HDAC4, HDAC5, HDAC7, HDAC9), class IIb (HDAC6, HDAC10), and class IV (HDAC11), which are related to yeast *Rpd3*,

doi:10.6342/NTU202500611

Had1, and *Hos3*. Class III (Sirtuins: SIRT1–SIRT7) corresponds to NAD^+-dependent yeast Sir2 homologs (de Ruijter et al., 2003; North et al., 2003).

In *Arabidopsis thaliana*, 12 RPD3/HDA1-type HDACs are grouped into three classes based on sequence similarity to mammalian HDACs: class I (HDA6, HDA7, HDA9, HDA10, HDA17, HDA19), class II (HDA5, HDA8, HDA14, HDA15, HDA18), and class IV (HDA2; Alinsug et al., 2009). Recombinant *Arabidopsis* HDA19, HDA5, and the HD domain of HDA18 expressed in *Escherichia coli* have shown HDAC activity in vitro (Fong et al., 2006; Liu et al., 2014). Furthermore, specific amino acids (H276, H277, D313, H315, H316) of HDA15 are essential for its enzymatic activity and biological functions (Chen et al., 2020).

Functions of HDA5

Histone deacetylase 5 (HDA5) is a member of the RPD3/HDA1 family of histone deacetylases in *Arabidopsis thaliana*. These enzymes play a crucial role in modulating chromatin structure and gene expression by removing acetyl groups from histone proteins, leading to chromatin condensation and transcriptional repression (Luo et al., 2015).

HDA5 has been demonstrated to possess deacetylase activity and is involved in the regulation of flowering time. Mutants deficient in *HDA5* expression exhibit a late-

doi:10.6342/NTU202500611

flowering phenotype, which is associated with the upregulation of flowering repressor genes such as *FLOWERING LOCUS C* (*FLC*) and *MADS AFFECTING FLOWERING 1* (*MAF1*). This suggests that HDA5 represses these genes to promote flowering under appropriate conditions (Luo et al., 2015).

Additionally, HDA5 has been implicated in the plant's response to environmental stresses such as salt stress. Proteome-wide lysine acetylation profiling has identified substrate proteins of HDA5 and revealed new lysine acetylation sites that become hyperacetylated upon salt stress. This indicates that HDA5 plays a role in modulating protein acetylation in response to environmental stress, thereby contributing to the plant's adaptive mechanisms (Tilak et al., 2023).

Motivation and Objectives

HDA5 has been shown to participate in various developmental growth pathways and abiotic stress defense mechanisms, such as salt stress. According to the Arabidopsis microarray database, *HDA5* is induced by heat stress, suggesting a potential role in the heat shock response (HSR) pathway. Therefore, our first objective is to investigate whether HDA5 plays a functional role in the HSR pathway.

doi:10.6342/NTU202500611

Additionally, previous studies indicate that HDA5 is an active nucleus-cytoplasmic HDAC (Tilak et al., 2023). This raises the possibility that HDA5 interacts with partner proteins, such as heat shock factors (HSFs), to regulate the transcriptome during heat stress. Thus, our second objective is to determine whether HDA5 collaborates with HSFs or other proteins to modulate transcriptional regulatory during HS.

doi:10.6342/NTU202500611

Material and Methods

Plant Materials and Growth Conditions

Arabidopsis (*Arabidopsis thaliana*) Columbia ecotype (Col-0) was used as the wild-type (WT) plants. The mutant line *hda5-1* (SALK_007503) and *CaMV 35S*-driven lines *GFP-HDA5* and *HDA5-YFP-HA* in the WT background were provided from Dr. Kaqiang Wu of National Taiwan University. The homozygous background of the *hda5-1* was identified by PCR (Luo et al., 2015). HDA5 coding sequence (CDS) region was cloned into pCR™/GW/TOPO® then subcloned into two different vectors: pK7WGF2 and pEG101 to generate *35S::GFP-HDA5* and *35S::HDA5-YFP-HA* constructs, respectively. The progeny of F3 were further identified with qRT-PCR and western blotting and used for thermotolerance tests.

Plants were grown in growth chambers at 23°C with 16 h light/8 h dark with a light intensity of 80 to 100 μmol m^{-2} s^{-1}. Thermotolerance tests, protein abundance assays, ChIP-qPCR assays and nuclear-cytoplasmic fractionation were conducted using 1/2 Murashige and Skoog medium ($^1/_2$ MS, Sigma) medium with 1% sucrose and 0.8% agar (Millipore).

doi:10.6342/NTU202500611

DNA/RNA Preparation, cDNA Synthesis and qRT-PCR

For DNA isolation, seedlings were ground in liquid nitrogen and mixed with Edwards buffer. After centrifugation at 12,000 rpm for 10 min, the supernatant was mixed with equal amount of isopropanol (IPA) to precipitate DNA at -20°C for 1 h. The DNA pellet was washed with 75% ethanol one time and dissolved in deionized water.

Total RNA was extracted using TRIZOL reagent (Invitrogen) and TURBO DNA-free kit (Applied Biosystems). Fifty 7-day-old seedlings were ground in liquid nitrogen, mixed with 800 μL TRIZOL, followed by 200 μL chloroform. After centrifugation at 12000rpm for 20 min, the supernatant was precipitated with equal amount of isopropanol in new Eppendorf at -20°C for 2 h. After precipitation, centrifuged at 12,000 rpm for 20 min and removed the supernatant, the RNA pellet was washed with 75% ethanol three times and dissolved in pre-heated 55°C 35 μL DEPC-treated water. TURBO DNase treatment was performed, and cDNA synthesis was done using a reverse transcription kit (Applied Biosystems). qRT-PCR was conducted with iQ SYBR Green Supermix, using *PP2AA3* (*PP2A*; At1g13320) as the internal control. Data were analyzed using the $2^{-\Delta\Delta CT}$ method.

doi:10.6342/NTU202500611

Thermotolerance Tests

Fifty 5-d-old seedlings were grown on solid $^{1}/_{2}$ MS medium plates used for thermotolerance tests. Plates were equally heated in the water bath for basal thermotolerance (BT), short-term acquired thermotolerance (SAT), long-term acquired thermotolerance (LAT), as previously described (Charng et al., 2007). Photos and survival rates were captured and measured 10 days post-treatment, respectively. The survival rate was defined as the condition in which seedlings did not exhibit complete bleaching and continued to grow leaves after a 10-d recovery period.

Western Blot Analysis and Protein Abundancy Assay

A hundred 7- day old seedlings were collected and ground in liquid nitrogen, for non-reducing conditions, the powder was mixed with ice-cold protein extraction buffer (50 mM Tris-HCl, pH 7.5, 150 mM NaCl, 10 mM $MgCl_2$, 0.1% NP-40, 1 mM PMSF) supplemented with 1x protease inhibitor cocktail (Roche). The extract was centrifuged at 12,000 rpm for 15 min to obtain clear protein extracts. Protein concentration was determined using a detergent-compatible protein assay (Bio-Rad). After electrophoresis with 10% or 15% gels, the separated protein was transferred from the gel to a 0.45 μm Immobilon®-P PVDF Membrane (Millipore). The membrane was incubated in 10 ml

doi:10.6342/NTU202500611

methanol for 10 min. After transfer, the membrane was then washed with PBS/Tween buffer three times. Immunoblot analysis was performed with relevant antibodies diluted in blocking buffer.

To characterization of *HDA5* transgenic line, the Anti-GFP (ab290, Abcam) were used to detected the signal and Rubisco Large subunit (RbcL) was used as loading control. For protein abundancy assay, anti-GFP (ab290, Abcam), anti-acetyl-H3 (06-599, EMD Millipore) and anti-acetyl-H4 (06-866, EMD Millipore) primary antibody was used at a 1:5000 dilution, and the anti-actin (AS16-3141, Agrisera) and anti-HSP101 (AS08-287, Agrisera) antibody was used at 1:10000. Secondary antibodies were used at a 1:10000 dilution. Signals were detected using chemiluminescence HRP substrates (Millipore) and an Imaging System (iBright™ CL750, Invitrogen). ImageJ software was used to quantify protein abundance, and signals from three independent experiments were quantified.

Agro-Infiltration in *Nicotiana benthamiana* Leaves

The Agrobacterium strain containing the precise construct was incubated in 5 mL of liquid LB medium supplemented with 50μg/ mL kanamycin and 25μg/ mL rifampicin at 28°C in a shaking incubator overnight. The following day, the cultures were centrifuged at 4000 rpm for 10 minutes at 4°C to pellet the cells. The supernatant was discarded, and

doi:10.6342/NTU202500611

the pellet was washed with 6 mL of infiltration buffer. After washing, the mixture was centrifuged again under the same conditions, and the pellet was resuspended in 2 mL of infiltration buffer supplemented with 1 mM acetosyringone (AS). This suspension was incubated overnight at 28°C in a shaking incubator.

On the third day, the appropriate ratio of bacterial suspensions was mixed, centrifuged at 4000 rpm for 10 minutes at 4°C, and the pellet was resuspended in 2–4 mL of 10 mM $MgCl_2$ supplemented with 1 mM AS. The suspension was incubated for 3–6 hours at 28°C before infiltration.

Three-week-old *N. benthamiana* leaves were used for agro-infiltration. A 200 μL tip was used to create small holes on the abaxial side of the leaves, and a 1 mL needle-less syringe was used to inject the bacterial suspension into the leaves. After infiltration, the plants were incubated in the growth chamber at 25°C for 2 days for exogenous proteins to express.

Arabidopsis Mesophyll Protoplasts Isolation and Plasmid Transfection

Arabidopsis mesophyll protoplasts were prepared from the leaves of 3- to 5-week-old seedlings (Col-0, *35S::GFP-HDA5*, *35S::HDA5-YFP-HA*)grown on soil under short-day light conditions (12 h light/12 h dark, 80–100 μmol m^{-2} s^{-1}). The Tape-Arabidopsis

doi:10.6342/NTU202500611

protoplast extraction method was used as described by Lin et al. (2009). The enzyme solution was modified to contain 1.5% cellulose R10 and 0.4% macerozyme R10, without the addition of BSA. After isolation, the protoplasts were washed three times with W5 solution and counted using a microscope and cell counting slide. A total of 4×10^5 cells were transfected with 10,000 ng of each fusion construct using a PEG-calcium-mediated method. Following a 10-minute transfection period with precise vectors that needed in MMG solution, the reaction was suspended in 2 mL W5 solution and incubated for 10 minutes, followed by centrifugation at 100 × g for 3 minutes. The transfected protoplasts were then resuspended in 1 mL W5 and transferred to 2 mL Eppendorf tubes for overnight incubation at 22°C under light conditions.

Green signal of *35S::GFP-HDA5* transgenic line and yellow signal of transfected *35S::HDA5-YFP* in Col-0 protoplasts and its transgenic line were detected with GFP channel and YFP channel, respectively, via confocal microscope (TCS SP5, Leica) in 40X oil lens. The NLS-mCherry was used as nuclear marker. Red signal was captured as the auto- fluorescence of chloroplast.

Bimolecular Fluorescence Complementation (BiFC) Assay

pEarlyGate201-YFP^N and pEarlyGate202-YFP^C vectors were used for BiFC analysis. Agrobacterium expressing HDA5-Y^N/ HSFs-Y^C (HSFs as described here was

doi:10.6342/NTU202500611

not including HSFB3 and HSFB4) were infiltrated into *N. benthamiana* leaves and incubated for 48 h. The signals were detected using fluorescence microscope in 40X lens. NLS-mCherry was used for nucleus marker.

For BiFC analysis in *Arabidposis* mesophyll protoplasts, HDA5-Y^N and HSFB2b-Y^C were both transfected into protoplast using PEG-mediated method. Reconstituted YFP signal was detected via confocal microscope (TCS SP5, Leica) in 40X oil lens. NLS-mCherry was used as the nucleus marker. The red signal represented as auto- fluorescence of chloroplast.

Yeast Two Hybrid (Y2H)

The pGBKDT7 (BD) and pGADT7 (AD) vectors along with yeast strains AH109 (-Leu) and Y187 (-Trp) were used for the analysis. Given that HSFs possess intrinsic DNA-binding and activation domains, we transformed the HSFs-AD and HDA5-BD gene-containing vectors into the yeast strains AH109 and Y187, respectively.

After selecting on single amino acid-deficient plates, yeast cells were incubated in YDPA broth overnight for mating with the specific combinations used for the final experimental setup. The concentration of mating yeast cells was adjusted to an OD of 0.6

doi:10.6342/NTU202500611

(1x) and diluted to 10^{-1} and 10^{-2} for growth on non-selective medium (-Leu, -Trp) or selective medium (-Leu, -Trp, -His) for 7 days.

Split-Luciferase Complementation Imaging (LCI) Assay

pGWB-nLuc and pGWB-cLuc vectors were used for this experiment. Full- length of *HDA5* were cloned into pGWB-nLuc via Gateway system. For *HSFA1d, HSFA8, HSFA9* and *HSFB2b*, full- length of CDS were cloned into pGWB-cLuc with same method. Plasmids were transformed into Agrobacteria GV3101, and the cells were combined and then injected into tobacco cells via agroinfiltration.

Luminescence signals were detected via imaging system (iBright™ CL750, Invitrogen). ImageJ was used for colored the strength of luminescence signals. Scale of 16 colors is represented as from weak (black) to strong (white) luminescence signals.

Nuclear-Cytoplasmic Fractionation

The sucrose gradient method, as described by Qi et al. (2011), was used for nuclear-cytoplasmic fractionation. One hundred 7-day-old *35S::HDA5-YFP* transgenic line seedlings were ground in liquid nitrogen. The resulting fine powder was mixed with lysis buffer (20 mM Tris-HCl, pH 7.5, 20 mM KCl, 2 mM EDTA, 2.5 mM $MgCl_2$, 25%

doi:10.6342/NTU202500611

glycerol, 250 mM sucrose, and 5 mM DTT) supplemented with 1x protease inhibitor cocktail (Roche). 50 μL of the homogenate were taken as the total protein extract. The remaining homogenate was filtered through a double layer of Miracloth (Millipore) and centrifuged at 1,500 × g for 10 minutes at 4°C to separate the cytosolic fraction containing supernatant and nucleus fraction containing pellet.

The supernatant containing the cytosolic fraction was transferred to a new Eppendorf tube and centrifuged again at 10,000 × g for 10 minutes at 4°C to collect the supernatant as the clean cytosolic fraction. The pellet containing nucleus fraction was washed four times with 1 mL of nuclear resuspension buffer NRBT (20 mM Tris-HCl, pH 7.4, 25% glycerol, 2.5 mM $MgCl_2$, and 0.2% Triton X-100) and then resuspended in 500 μL of NRB2 (20 mM Tris-HCl, pH 7.5, 0.25 M sucrose, 10 mM $MgCl_2$, 0.5% Triton X-100, and 5 mM β-mercaptoethanol) supplemented with 1x protease inhibitor cocktail (Roche). The sample was carefully overlaid onto 500 μL of NRB3 (20 mM Tris-HCl, pH 7.5, 1.7 M sucrose, 10 mM $MgCl_2$, 0.5% Triton X-100, and 5 mM β-mercaptoethanol) supplemented with 1x protease inhibitor cocktail (Roche) and centrifuged at 16,000 × g for 45 minutes at 4°C. The final nuclear pellet was resuspended in 100 μL of lysis buffer. Western blotting was conducted to detect the signals. Anti-GFP (ab290, Abcam) was used

doi:10.6342/NTU202500611

for probed the HDA5-GFP. Histone H3 (06-755, EMD Millipore) was probed and used as a nuclear marker.

Chromatin Immunoprecipitation (ChIP)-qPCR

For ChIP-qPCR, ChIP was carried out as described by Colot et al. (2005). A total of seven to eight hundreds of 7-day-old seedlings were grown on 0.8% agar containing ½ MS medium in growth chambers at 23°C under a 16 h light/8 h dark cycle with a light intensity of 80–100 μmol m^{-2} s^{-1}. Seedlings, either treated or untreated with 37°C in a water bath, were fixed with 37 mL of 1% formaldehyde for crosslinking under vacuum for 15 minutes, repeated twice. After crosslinking, 2.5 mL of 2M glycine was added to quench the reaction, followed by vacuuming for 5 minutes. Samples were then frozen in liquid nitrogen and stored at -80°C until use.

Tissues were ground into fine powder and extracted with extraction buffers 1, 2 and 3. After extraction, the pellet containing the DNA was resuspended in 400 μL of nuclei lysis buffer for further fragmentation. Sonication (SONICS; Catalogue no. VCX130) was performed to shear the DNA, and fragment size was confirmed to be less than 1000 bp by PCR. After centrifugation at 12,000 rpm for 10 minutes, 4 μL of the supernatant was saved as the input sample. The remaining supernatant was immunoprecipitated overnight

doi:10.6342/NTU202500611

at 4°C using the anti-H3 (06-755, EMD Millipore), anti-acetyl-H3 (06-599, EMD Millipore), anti-acetyl-H3K9 (07-352, EMD Millipore) and anti-H3K4-dimethyl (ab7766, Abcam) antibody with gentle flat rotation. The DNA-protein-antibody complex was captured with Dynabeads Protein G.

Beads were washed, and DNA was eluted from the complex using elution buffer and incubated overnight at 55°C. After elution, the ChIP DNA was treated with proteinase K for 1 hour at 45°C in a dry bath. To separate the mixture, 275 μL of phenol-chloroform-isoamyl alcohol (PCI) was added. Following centrifugation at 12,000 rpm for 10 minutes, 250 μL of upper DNA-containing layer was transferred to a new Eppendorf tube and mixed with 2.5 μL of 3M sodium acetate, 2 μL of glycogen carrier, and 625 μL of 99% absolute ethanol. After overnight incubation at 4°C, the mixture was centrifuged at 12,000 rpm for 10 minutes to pellet the DNA. The pellet was resuspended in 35 μL of ddH_2O and stored at -20°C until further use.

ChIP-qPCR was conducted with iQ SYBR Green Supermix, using *ACT2* (At3g18780) and H3 as the internal control. Data were analyzed using the $2^{-\Delta\Delta CT}$ method.

doi:10.6342/NTU202500611

Dual Luciferase Reporter (DLR) Assay

HSFB2b-Y^N and HDA5-Y^N were used as the effectors. For empty vector, Ev-Y^N was used. For reporters, a size of 1.5 kb promoter region of *HSP22* loci was cloned into pGreenII 0800-Luc. The concentrations of agrobacterium were calculated as equal amounts for each combination before infiltration. All data were normalized to REN.

doi:10.6342/NTU202500611

Results

Gene Expression Patterns of Arabidopsis *HDA5* Under Heat Stress Conditions

To investigate the expression levels of Arabidopsis *HDA5* in response to heat stress, we grew fifty 7-day-old Col-0 seedlings on 1/2 MS plates for treatment and used them for qRT-PCR analysis. The heat-inducible gene *HSP18.2* were served as a positive control.

The qRT-PCR results showed no significant difference *HDA5* expression levels at any time point compared to the Col-0 control **(Figures 1C and 1D)** in either the BT test or the SAT test **(Figure 1A and 1B)**, indicating that HDA5 is not a HS-responsive gene in HS condition.

Characterization of the *hda5* Knock-out Line and pCaMV *35S*/ *HDA5* Native Promoter-Driven *HDA5* Transgenic Lines

To investigate the function of HDA5, we confirmed the *hda5* knockout line (SALK_007503) provided by Dr. Kaqiang Wu at National Taiwan University, as described by Luo et al. (2015) **(Figure 2A)**. After receiving the seeds, we amplified them and conducted a RT-PCR analysis. The results confirmed the absence of the HDA5 transcript in the *hda5* mutant, validating it as a knockout line **(Figure 2B)**.

doi:10.6342/NTU202500611

To characterize the transgenic lines driven by the *pCaMV 35S* and native *HDA5* promoters **(Figure 3B)**, we performed qRT-PCR **(Figure 3A)** on F3 progeny. The results showed that the transgenic lines *35S::GFP-HDA5* (cloned in pK7WGF2 vector) and *35S::HDA5-YFP-HA* (cloned in pEG101 vector) exhibited significantly higher expression than Col-0, with increases ranging from 100-120 folds and 15-30 folds **(Figure 3C)**, respectively. In the complementation lines with native promoter-driven *HDA5* in the *hda5* mutant background, *HDA5* expression was slightly lower than in Col-0 **(Figure 3C)**, which may indicate functional compensation. Western blotting with a GFP antibody confirmed the tagged constructs, with the molecular weight of the HDA5-GFP fusion protein being approximately 100 kDa **(Figure 3D)**.

hda5-1 Shown Insensitive Phenotypes Toward Multiple HS Conditions

To verify the role of HDA5 in regulating plant physiological functions under heat stress, we conducted basal and acquired thermotolerance tests using 5-day-old seedlings of *hda5-1*, *35S::GFP-HDA5* (*#1*), *35S::HDA5-YFP* (*#1.2*), and Col-0. The heat-sensitive mutant *hsp101* was used as a reference.

In the BT tests **(Figure 4)**, lethal heat stress durations of 24, 26, and 28 minutes were applied at 44°C. The *hsp101* mutant had a survival rate of about 1%, highlighting its

doi:10.6342/NTU202500611

extreme heat sensitivity. In contrast, Col-0 survival rates dropped from 35–40% at 24 minutes to 15–23% with extended heat stress, indicating that 24–28 minutes is sufficient to assess thermotolerance in Arabidopsis. The *hda5-1* mutant showed significantly higher survival rates than Col-0 at 24 and 26 minutes. However, by 28 minutes, this difference diminished, suggesting a limit to HDA5's effectiveness under prolonged heat stress. Overexpression (OE) lines *35S::GFP-HDA5* (#1) and *35S::HDA5-YFP* (#1.2) did not significantly differ from Col-0, except for a slightly lower survival rate at 24 minutes.

To evaluate the role of HDA5 in acquired thermotolerance, both SAT and LAT tests were performed. For the SAT tests **(Figure 5)**, 5-day-old seedlings were primed at 37°C for 1 hour, allowed to recover at 22°C for 2 hours, and then exposed to lethal heat stress at 44°C for 180 and 190 minutes. These treatments resulted in survival rates of approximately 50% for Col-0 and around 1% for *hsp101* plants. In contrast, the *hda5-1* mutant showed significantly higher survival rates, especially after 190 minutes, indicating the involvement of HDA5 in short-term acquired thermotolerance. Notably, the OE lines *35S::GFP-HDA5* (#1) and *35S::HDA5-YFP* (#1.2) exhibited survival patterns that were opposite to those of Col-0 and *hda5-1*, which correlated with the results from the BT test (24-minute lethal heat stress duration) **(Figure 4)**.

doi:10.6342/NTU202500611

In the LAT tests **(Figure 6)**, 5-day-old seedlings were primed at 37°C for 1 hour, allowed to recover for 2 days, and then exposed to lethal heat stress for shorter durations of 85, 95, and 105 minutes at 44°C. The survival rates for Col-0 and *hsp101* decreased from 40–50% to 20–25% and from 4% to 0%, respectively. Although the *hda5-1* line showed no difference in survival compared to Col-0 at 85 minutes, it exhibited significantly higher survival rates at the 95 and 105-minute marks.

In accordance with the results seen in BT and SAT **(Figure 4 and 5)**, the OE lines *35S::GFP-HDA5* (#1) and *35S::HDA5-YFP* (#2) showed significantly lower survival rates than Col-0 during the 85, 95, and 105-minute treatments, respectively. These findings indicate that HDA5 may play a role in maintaining protein homeostasis under heat stress conditions.

In summary, our results suggest that HDA5 acts as a negative regulator of heat stress responses, influencing both basal and acquired thermotolerance in Arabidopsis.

Interactions Between HDA5 and Heat Shock Factors (HSFs).

To investigate potential interaction partners of HDA5 during heat stress, we performed a BiFC assay with various HSFs. We expressed HDA5-Y^C along with 19 HSFs-Y^N constructs (excluding HSFB3 and HSFB4) in *N. benthamiana* cells. We found

doi:10.6342/NTU202500611

nuclear interactions between HDA5 and HSFA1d, HSFA8, HSFA9, and HSFB2b in the nucleus **(Figures 7A-C; Supplemental Fig. 1)**. HSFA2-Y^N and HSFC1-Y^C interaction acted as a positive control observed in the nucleus **(Figure 7D)**, while HDA5-Y^C/Ev-Y^N and HSFs-Y^N/Ev-Y^C served as negative controls **(Figure 7E)**.

To further confirm the interactions, LCI and Y2H assays were also conducted. For the LCI assay **(Figure 8)**, each *N. benthamiana* leaf was divided into four sections for injection. Recombinant luminescence was successfully detected in the sections injected with HDA5-nLuc, as well as with HSFA1d-cLuc, HSFA8-cLuc, HSFA9-cLuc, or HSFB2b-cLuc, and the signal intensity was quantified using ImageJ software. For the negative controls, no luminescence was detected throughout the experiment.

In the Y2H assay **(Figure 9)**, the mating yeast cells were cultivated on two types of media: a non-selective medium (-Leu, -Trp) and a selective medium (-Leu, -Trp, -His) for a period of 7 days. Successful yeast mating was confirmed by the continued growth of all mating combinations on the non-selective medium. On the selective medium, interactions between the target proteins activated the *HIS3* gene, enabling the yeast to survive in the His-deficient environment.

doi:10.6342/NTU202500611

Colony growth demonstrated interactions between HDA5 and the proteins HSFA1d, HSFA8, and HSFA9. However, self-activation was noted for the HDA5-BD and Ev-AD combination on the selective medium, where the yeast exhibited slow growth after 7 days due to partial activation of *HIS3*. In contrast, colonies with HDA5-BD/HSFA1d-AD, HSFA8-AD, and HSFA9-AD grew more rapidly than the self-activating control, indicating full activation of *HIS3*.

The combination of HDA5-BD and HSFB2b-AD exhibited slower growth compared to the self-activating control. This suggests that HSFB2b may inhibit *HIS3* activation through its interaction with HDA5. It is possible that HDA5 activates HSFB2b, which is a transcriptional repressor, and this activation then leads to the repression of *HIS3*.

In conclusion, HDA5 interacts with HSFA1d, HSFA8, HSFA9, and HSFB2b.

Gene Expression Profiles of HS- Responsive Genes in *hda5-1*.

To test if the HDA5 partner with HSFs to regulates HSR genes, we performed qRT-PCR to analyze gene expression in *hda5-1* and Col-0 during both basal **(Figure 10A)** and short-term acquired thermotolerance **(Figure 11A)** tests. Under BT conditions, several genes, including *HSFA2*, *HSFA7a*, *HSFA7b*, and *HSP101*, were mildly upregulated in *hda5-1* when compared to Col-0 **(Figure 10B).**

doi:10.6342/NTU202500611

In the AT test **(Figure 11A)**, mild pre-treatment at 37°C effectively primed the plants to respond rapidly to subsequent higher stress. Several HSF and HSP genes were upregulated following priming stress. Notably, the master regulator *HSFA2* did not show significant differences compared to Col-0, while its partner *HSFA3* was significantly upregulated. HSPs such as *HSP18.2*, *HSP22*, and *HSP101* were also upregulated throughout the heat stress treatment **(Figure 11B)**. These results suggest that the loss of HDA5 alters the regulation of key components in the HSR.

We also examined the expression of *HDA18*, a potential functional partner of HDA5, which has been previously implicated in the salt stress response (Tilak et al., 2023). Due to the shared sequence similarity between *HDA5* and *HDA18* in their conserved domains, *HDA18* was found to be upregulated in *hda5-1* under heat stress compared to Col-0. This suggests that HDA18 may partially compensate for the loss of HDA5 during heat stress.

Accumulation of HSP101 and Acetyl-H3 Levels in *hda5-1* During Heat Stress

To validate the qRT-PCR results, we treated 100 seven-day-old seedlings with mild heat stress at 37°C for 1-3 hours to activate the HSR. We also included a recovery group exposed to 37°C for 1 hour followed by 1 hour at 22°C **(Figure 12A)**. In control

doi:10.6342/NTU202500611

conditions, HSP101 levels were low in Col-0, while *hda5-1* seedlings exhibited approximately two-fold higher levels **(Figure 12B)**.

After priming stress at 37°C for 1 and 3 hours, HSP101 expression increased 9.1-fold and 19.1-fold in Col-0, while in *hda5-1*, it increased 13.8-fold and 30.8-fold, respectively. In the recovery group (1 hour of heat stress followed by 1 hour of recovery), HSP101 increased 12.1-fold in Col-0 and 20.8-fold in *hda5-1*, which is 1.7 times higher than in Col-0. These results suggest that HDA5 regulates HSP101 expression, in both CK and HS conditions.

As expected, *hsp101* mutant lines, serving as a heat-sensitive control, exhibited notable deficiencies in thermotolerance **(Figures 4, 5, and 6)**, highlighting the essential role of HSP101 in the HS response of Arabidopsis.

In this experiment, we measured genome-wide levels of total acetyl-H3. In the Col-0 strain, acetyl-H3 levels increased by about 1.26-fold during the first hour of heat stress. The *hda5-1* strain showed even higher acetyl-H3 levels in response to early heat stress, indicating that multiple genes were rapidly acetylated without the deacetylation activity of HDA5. After 3 hours of priming stress, acetyl-H3 levels in both strains became

doi:10.6342/NTU202500611

comparable, highlighting that the differences were most notable in the initial phase of the HSR.

Interestingly, in the recovery group, the *hda5-1* maintained slightly higher levels of acetyl-H3 compared to the Col-0. This observation suggests that the HSR in *hda5-1* may be activated more quickly, even in a non-stress environment, allowing for more effective management of cellular stress.

Throughout the experiment, anti-actin was used as an internal control, as its expression remained stable and was unaffected by heat stress.

Based on these findings, we propose that HDA5 directly regulates multiple HS-responsive genes under heat stress conditions. In particular, the qRT-PCR results highlight *HSP22* and *HSP101* as key targets for further investigation into the regulatory role of HDA5.

HDA5 Participating in the Regulation of the *HSP18.2, HSP22* and *HSP101* Loci in HS

To determine whether HDA5 regulates the *HSP18.2, HSP22* and *HSP101* loci, we performed ChIP-qPCR analysis on Col-0 and *hda5-1* plants following genome-wide

doi:10.6342/NTU202500611

acetyl-H3 results **(Figure 12)**. The plants were subjected to 1 hour of heat stress at 37°C, followed by 1 hour of recovery at 22°C **(Figures 13B, 14B, and 15B)**.

The results indicated that the levels of acetylated H3 at the transcription start site (TSS) of *HSP22* **(see Figure 14A and C's amplicon 1)**, which contains two HSE motifs, were elevated under both control and heat recovery conditions. An amplicon designed from the 400-bp region upstream of the TSS **(see Figure 14A and C's amplicon 2)**, which also includes two HSE motifs, demonstrated increased acetyl-H3 levels during the heat recovery stage. In contrast, for *HSP101* **(see Figure 15A and 15C's amplicon 1)**, which lacks HSE motifs, an amplicon approximately 150 bp upstream of the TSS showed no significant changes in acetyl-H3 levels due to the absence of HDA5.

Further analysis revealed that H3K9 acetylation levels at the *HSP22* loci were significantly elevated in the *hda5-1* mutant during the heat recovery stage at the TSS **(see Figure 14A and D's amplicon 1)**. Additionally, during the heat stress stage, there was an increase in acetylation levels 400 bp upstream of the TSS **(see Figure 14A and D's amplicon 2)**. However, under control (CK) conditions, acetylation levels were downregulated at the 400 bp upstream TSS.

doi:10.6342/NTU202500611

Previous studies have demonstrated an antagonistic relationship between H3K9 acetylation (H3K9ac) and H3K4 dimethylation (H3K4me2) in Arabidopsis HDA5 (Luo et al., 2015). Consistent with this, we observed that in the *hda5-1* mutant, H3K4me2 levels were downregulated at the TSS amplicon during the heat recovery stage, while H3K9ac levels were upregulated **(see Figure 14D and 14E's amplicon 1)**. In contrast, at the 400 bp upstream TSS, H3K4me2 levels were upregulated and H3K9ac levels were downregulated **(see Figure 14D and 14E's amplicon 2)**.

Interestingly, when comparing H3K4me2 levels in the *hda5-1* mutant to those in Col-0, the patterns were nearly opposite at all stages and amplicons **(Figure 14E)**. This suggests that histone methylation plays a crucial role in regulating *HSP22* under HS.

In *HSP101*, H3K9ac levels showed no significant difference between *hda5-1* and Col-0 **(Figure 15D)**. In contrast, H3K4me2 levels were oppositely regulated at the control (CK) and heat recovery (HR) stages in *hda5-1* compared to Col-0 **(Figure 15E)**.

We also investigated the *HSP18.2* loci, specifically focusing on an amplicon designed at the 5'-UTR **(see Figure 13A amplicon 1)**. Similar to the results observed in *HSP101*, the levels of acetylation were not significantly affected by the loss of HDA5

doi:10.6342/NTU202500611

(Figure 13C and D). However, the levels of H3K4me2 were regulated in the opposite manner in the *hda5-1* mutant compared to the Col-0 plants **(Figure 13E)**.

In summary, HDA5 may directly regulate *HSP22*, emphasizing the role of histone methylation in the HSR.

HDA5 Is Relocated from the Nucleus to the Cytosol under Heat Stress Conditions.

Previous studies revealed that HDA5 functions as a dynamic HDAC that shuttles between the cytosol and nucleus under salt stress (Tilak et al., 2023). To investigate its localization under HS, we isolated mesophyll protoplasts from *Arabidopsis* Col-0, *35S::GFP-HDA5*, and *35S::HDA5-YFP* plants. For Col-0, the *35S::HDA5-YFP* vector was used for transfection **(Figures 16A-C)**.

The results of the subcellular localization study showed that under normal conditions, HDA5 was found in the cytosol and partially co-localized with the nuclear marker NLS-mCherry in all three types of mesophyll protoplasts. However, after heat stress (HS) treatment lasting from 30 minutes to 1.5 hours, HDA5 was no longer detected in the nucleus. Interestingly, HDA5 formed speckle-like aggregates around the nucleus. Based on their localization, we suggest that these speckles are associated with the endoplasmic reticulum (ER) **(see Figure 16B and C)**.

doi:10.6342/NTU202500611

To confirm subcellular localization, we conducted nuclear-cytoplasmic fractionation **(Figure 17)**. The results showed that the *35S::HDA5-YFP* signal was detected only in the nucleus under control conditions, reinforcing the observations from the mesophyll protoplast localization analysis.

HDA5 and HSFB2b Repress the Transcriptional Activity of *HSP22*.

Given that HDA5 is absent from the nucleus during the HSR, we hypothesized it may activate HSFB2b through deacetylation. We cloned a 1.5 kb promoter region of HSP22 into pGreenII 0800-Luc as a reporter **(Figure 18A)**.

The dual-luciferase reporter (DLR) results showed that HSFB2b-Y^N alone did not affect HSP22 transcriptional activity. However, when both HSFB2b-Y^N and HDA5-Y^N were present, the expression level of *HSP22* was significantly downregulated. This suggests that HDA5 may activate HSFB2b via deacetylation, leading to repression of *HSP22* transcription **(Figure 18B)**.

doi:10.6342/NTU202500611

Discussion

HDA5 Functions as a Negative Regulator in HSR.

Previous studies indicate that HDA5 is involved not only in developmental growth but also in response to abiotic stresses (Luo et al., 2015; Tilak et al., 2023). Arabidopsis microarray database (AtGenExpress consortium) indicates that heat stress induces *HDA5*. However, our results show that the expression of *HDA5* does not change significantly in Col-0 during basal and short-term thermotolerance tests **(Figure 1)**. This suggests that HDA5 is not a HS-responsive gene.

We further investigated the basal thermotolerance as well as short-term and long-term acquired thermotolerance in the *hda5-1* mutant and its OE lines. The *hda5-1* mutant exhibited a less sensitive phenotype in all three types of thermotolerance tests **(Figures 4, 5 and 6)**, suggesting its negative role in HSR.

Previous studies have indicated that HDA5 can deacetylate both histone and non-histone proteins (Tilak et al., 2023). Our results indicate that HDA5 levels remain stable throughout the HSR in Col-0, as its expression does not change significantly **(Figure 1)**. Based on enzyme kinetics, this suggests that HDA5 may become saturated if its substrates include not only histone proteins, which are relatively stable in quantity (since the number

doi:10.6342/NTU202500611

of DNA octamers is fixed throughout the life cycle), but also HSR proteins, which are dramatically induced under HS conditions.

Interestingly, if the *HDA5* OE lines exhibited similar survival rates compared to Col-0, this would suggest that HDA5 targets only histone proteins, leading to fewer available substrates and preventing HDA5 saturation. However, we observed that *HDA5* OE lines displayed a survival pattern opposite to that of the *hda5-1* mutant and Col-0 **(Figures 4, 5, and 6)**. This suggests that HDA5 deacetylates not only histone proteins but also HSR proteins. The dynamic nature of HSR proteins may saturate the intrinsic HDA5 in Col-0, causing the reaction rate of HDA5 to approach its threshold due to a dramatic increase in substrate levels (enzyme kinetics). On the other hand, *HDA5* OE lines can process more substrates to 'turn off' the HSR response due to the increased numbers of HDA5, leading to lower survival rates compared to Col-0 and *hda5-1*.

Unfortunately, we were unable to investigate this hypothesis further due to the late emergence of these phenotypes, which required additional replicates and expanded stress durations. These observations coincided with the timing of our Y2H and DLR assays, which are discussed below.

doi:10.6342/NTU202500611

HDA5-Mediated Regulation of Heat Shock Factors (HSFs) and Heat Shock Proteins (HSPs) Across Multiple Pathways.

Although RNA-seq analysis was not performed, qPCR results revealed that *hda5-1* mutants exhibited significantly higher expression levels of several *HSFs and HSPs* compared to Col-0 during basal thermotolerance and short-term acquired thermotolerance **(Figure 10 and 11)**.

For BT test, *HSFA2*, *HSFA7a*, *HSFA7b* and *HSP101* were mildly upregulated in *hda5-1* **(Figure 10)**, however, this upregulation was less pronounced compared to the acquired thermotolerance response **(Figure 11)**. This suggests that in the absence of prior mild heat exposure (37°C), the transcriptome is not fully activated to handle lethal heat stress (44°C). The higher survival rate of *hda5-1* in the basal thermotolerance test **(Figure 4)**, compared to Col-0, is likely not due to changes in gene expression but rather to the un-deacetylation of internal non-histone proteins.

In the SAT test, several genes were significantly increased in *hda5-1*, when compared to Col-0, these genes included *HSFA1d, HSFA3, HSFA7a, HSP18.2*, *HSP22*, *HSP70-B*, and *HSP101* **(Figure 11)**.

HSFA1d, a member of the HSFA1 subclass, functions as a key initiator of the HSR, working redundantly with HSFA1a and HSFA1b to regulate downstream *HSFs* and *HSPs*

doi:10.6342/NTU202500611

expressions (Lohmann et al., 2004). HSR is triggered by multiple signaling pathways, including accumulation of reactive oxygen species (ROS) and calcium particles (Ca^{2+}), which induced DREB2A and HSFA8 (Giesguth et al., 2015). *HSFA3* expressions is induced by DREB2A, which form the HSFA2/HSFA3 trimers to act as the master regulators of HSR. Although we did not investigate whether HDA5 interacts with DREB2A, our study revealed that HDA5 interacts with HSFA1d and HSFA8 **(Figure 7A, 8 and 9)** and the significantly upregulated *HSFA3* expression in *hda5-1* **(Figure 11)**, suggesting a potential role in repressing early HSR via multiple pathways by targeting non-histone proteins.

HSFA9 plays a pivotal role in seed longevity by activating the expression of specialized *HSPs* during the late stages, with its functions extending into 10-day-old seedlings, including contributions to the basal thermotolerance (Tejedor-Cano et al., 2010). Our study revealed an interaction between HDA5 and HSFA9 **(Figures 7A, 8 and 9)**; however, the precise mechanism underlying this interaction remain unclear. Notably, basal thermotolerance tests showed that the absence of HDA5 (*hda5-1* mutant) resulted in a significantly higher survival rate when compared to Col-0 **(Figure 4)**. These findings

doi:10.6342/NTU202500611

suggest that HDA5 may inactivate HSFA9, acting as a negative regulator in seed longevity and basal thermotolerance.

As for the downstream HS-responsive genes, HDA5 repress the expression of key *HSPs*, including *HSP18.2, HSP22, HSP70-B* and *HSP101*, which play critical roles in thermotolerance and stress adaptation. Among these genes, *HSP18.2* belongs to the sHSP-CI subfamily, which consists of six functionally redundant genes. *HSP22* is a crucial sHSP localized in the ER, where it plays a key role in managing ER stress. *HSP101* is the most significant HSP localized in the cytosol during the HSR. The loss-of-function mutant of *HSP101* is commonly used as a heat-sensitive model in thermotolerance tests **(Figures 4, 5 and 6)**.

To confirm whether the upregulated transcript expression in *hda5-1* affects protein abundance, we used an anti-HSP101 antibody, to assess protein accumulation in *hda5-1* and Col-0. Our results showed that HSP101 levels in *hda5-1* were at least 1.5-fold higher than in Col-0 under both control and heat stress (HS) conditions **(Figure 12)**. These findings are consistent with the upregulated *HSP101* expressions **(Figure 11)** and the patterns of H3K4me2 levels at the *HSP101* loci in *hda5-1* **(Figure 15E)**.

doi:10.6342/NTU202500611

Further analysis of acetyl-H3 levels in *hda5-1* and Col-0 revealed that acetyl-H3 levels were higher in *hda5-1* during both heat stress and heat recovery stages compared to Col-0. These results suggest that HDA5 may regulate the loci of *HSP* genes by interacting with specific HSFs in early HSR and heat recovery process.

In conclusion, these findings suggest that HDA5 regulates through multiple regulatory pathways, impacting HSFs and downstream *HSP*s expressions to repressing the HSR. This multifaceted regulation likely involves direct interactions with HSFs and indirect effects mediated by non-histone protein deacetylation or chromatin remodeling. Further studies are required to fully elucidate the complex network of HDA5-mediated pathways in plant HSR.

Along with the downstream genes of HSR, *HSP18.2*, *HSP22* and *HSP101* were the most significantly upregulated throughout the whole treatment **(Figure 11)**, we mainly focus on these three downstream HSR genes in the HDA5-mediated HSR pathway.

HDA5 Interacts with HSFB2b.

HDACs, including HDA5, do not possess intrinsic DNA-binding domains, yet changes in gene expression have been observed in the absence of HDA5. This observation led us to hypothesize that certain HSFs might direct HDA5 to heat stress (HS) gene loci

doi:10.6342/NTU202500611

by recognizing HSEs. Among the 19 identified HSFs, we found that HDA5 interacts with HSFA1d, HSFA8, HSFA9, and HSFB2b in the nucleus **(Figures 7A, 8, and 9)**. The HSFA class contains an AHA domain, which primarily acts as a transcriptional activator. In contrast, the HSFB class lacks the AHA domain and is generally regarded as a class of transcriptional repressors (Nover et al., 2001). Previous studies have demonstrated that HSFB2b functions as a transcriptional repressor in various regulatory pathways, particularly in the regulation of acquired thermotolerance (Ikeda et al., 2011). Since both HDA5 and HSFB2b act as negative regulators of the HSR, we hypothesize that they may collaborate to "turn off" the HSR during heat stress conditions.

HDA5 Affects the Histone Modifications of *HSP18.2, HSP22* and *HSP101* loci.

A previous study indicated that HDA5 hyperacetylates H3K9 and H3K14, negatively regulating H3K4me2 levels at several genes associated with flowering, which leads to a late-flowering phenotype (Luo et al., 2015). Building on this concept, we investigated the levels of H3 acetylation, H3K9 acetylation, and H3K4me2 at the *HSP18.2, HSP22,* and *HSP101* loci in both *hda5-1* mutants and the Col-0 **(Figures 13, 14, and 15)**.

doi:10.6342/NTU202500611

The results indicated that there were no changes in the levels of H3ac or H3K9ac at the *HSP18.2* and *HSP101* loci. This suggests that HDA5 indirectly regulates these genes under HS conditions. Conversely, at the *HSP22* loci, acetylation levels were significantly increased at both the transcription start site (TSS) and 400 bp upstream of the TSS in all conditions (control, heat stress, and heat recovery) in the *hda5-1* strain compared to the Col-0 strain. This suggests that HDA5 may directly regulate the *HSP22* gene.

Interestingly, the patterns of H3K4me2 levels at *HSP18.2*, *HSP22*, and *HSP101* loci in *hda5-1* were completely opposite to those in Col-0 (**Figures 13E, 14E, and 15E)**. Furthermore, an antagonistic relationship between H3K9ac and H3K4me2 was observed at the *HSP22* loci, specifically at the TSS during HR stages and at the site 400 bp upstream of the TSS in control stages (**Figures 13D and E)**. These findings broaden the scope of HDA5's role in the regulation of the HSR pathway.

HDA5 Completely Relocated Outside the Nucleus During HS.

We hypothesized that HSFB2b might guide HDA5 to HSR genes loci by recognizing HSEs. Previous studies also reported that HDA5 exhibits a nucleus-cytoplasmic shuttling property. However, subcellular localization experiments in protoplasts and nuclear-cytoplasmic fractionation assays revealed that HDA5 was present in the nucleus only

doi:10.6342/NTU202500611

under optimal conditions and completely relocated to the cytoplasm during HS **(Figures 16 and 17)**.

HDA5 May Activates HSFB2b to Repress the HSP22 via Deacetylation.

The initial hypothesis that HDA5 works with HSFB2b to directly regulates HSR genes loci during HS was proven incorrect, which led us to investigate whether HDA5 activates HSFB2b through deacetylation. Around this time, we successfully conducted yeast two-hybrid assays **(Figure 9)** and dual-luciferase reporter assays **(Figure 18)**. Both sets of results supported our revised hypothesis that HDA5 activates HSFB2b to repress the transcriptional activity of *HSP22* through deacetylation.

In the yeast two-hybrid assay **(Figure 9)**, the interaction between HDA5-BD and HSFB2b-AD led to partial activation of the *HIS3* gene, resulting in slower yeast growth compared to the auto-activated HDA5-BD/Ev-AD. This finding suggests that HDA5 may activate HSFB2b to inhibit transcriptional activity. Although we considered the possibility that HSFB2b could direct HDA5 to specific gene loci for transcriptional repression, this hypothesis fails to account for the self-activation observed with HDA5-BD/Ev-AD.

doi:10.6342/NTU202500611

Further investigation into the regulatory partnership between HDA5 and HSFB2b revealed that their combined presence on led to transcriptional repression of *HSP22* **(Figure 18)**. Similar results also found, HDA5 alone on promoter regions resulted in transcriptional activation, while HSFB2b alone did not affect transcriptional activity. Together, these findings suggest that HDA5 might activates HSFB2b for transcriptional repression via deacetylation.

HDA5 is Involved in Regulating Histone Modification-Related Proteins in HS.

Interestingly, although HDA5 translocated outside the nucleus during HS **(Figure 16 and 17)**, the acetylation levels at the *HSP22* loci are still affected when comparing *hda5-1* mutants to Col-0. This observation led us to consider a previous study suggesting that HDA5 may interact with HDA18 in response to salt stress (Tilak et al., 2023).

Both HDA5 and HDA18 belong to the type II HDACs in Arabidopsis, displaying enzymatic activity and sharing similar conserved domains and functions. Our study shows that in the *hda5-1* mutant, the expression of HDA18 is significantly higher than in Col-0 under both control and HS conditions **(Figure 11)**. Based on these findings, we hypothesize that HDA5 and HDA18 may exhibit functional redundancy in supporting optimal plant growth and responding to heat stress.

doi:10.6342/NTU202500611

Numerous studies have highlighted the cross-talk between histone methylation and histone acetylation; however, the precise mechanisms underlying this complex regulation remain elusive. Our findings reveal an antagonistic relationship between H3K9 acetylation (H3K9ac) and H3K4 dimethylation (H3K4me2) at the *HSP22* loci **(Figure 14D and E)**. Additionally, the opposite expression patterns of H3K4me2 on *HSP18.2* and *HSP101* loci in *hda5-1* compared to Col-0 **(Figure 13E and 15E)** suggests that HDA5 may be involved in regulating histone methylation, leading to the upregulated *HSP18.2* and *HSP101* expressions **(Figure 11)**.

Nevertheless, the mechanisms by which histone methylation contributes to HSR remain largely unexplored. These findings not only expand our understanding of HDA5's role in regulating the HSR pathways but also underscore the need for further investigation to unravel this complex regulatory network.

Perspective and Future Works

We hypothesize that HDA5 may activate HSFB2b through deacetylation, and several evidences support this mechanism **(Figure 19)**. However, additional data are required to validate this hypothesis. The first priority is to confirm that HDA5 directly deacetylates HSFB2b. Second, experiments utilizing the *hsfB2b* single mutant and the

doi:10.6342/NTU202500611

hda5/hsfB2b double mutant lines will be essential to further clarify the interaction between these proteins.

Additionally, to elucidate the role of HDA5 in regulating the initiation of the HSR, we plan to perform proteome-wide Lys-acetylation levels in Col-0, *hda5-1* and one of the *HDA5* OE line to confirm that HDA5 deacetylates the non-histone target proteins during HS.

In conclusion, HDA5 acts as a negative regulator in the HSR pathways. Its role in responding to heat stress likely extends beyond histone modification, as it primarily targets non-histone proteins, including HSFs and potentially proteins related to histone methylation.

doi:10.6342/NTU202500611

Tables

Table 1. List of primer sequences for cloning, RT-PCR, qPCR, and ChIP-qPCR

	Primer	Sequence (5’ to 3’)
Cloning		
HDA5	CDS-HDA5-Fw	ATGGCTATGGCCGGAGAATCT
	CDS-HDA5-Rv	GAGAGGTTTAGACACAGCCTTGTCTATGT
HSFA1a	CDS-HSFA1a-Fw	ATGTTTGTAAATTTCAAATACTTCTCTTTCTTTATCC
	CDS-HSFA1a-Rv	GTGTTCTGTTTCTGATGTGAGAAGACC
HSFA1b	CDS-HSFA1b-Fw	ATGGAATCGGTTCCCGAATCCGT
	CDS-HSFA1b-Rv	TTTCCTCTGTGCTTCTGAGGAAAG
HSFA1d	CDS-HSFA1d-Fw	ATGGATGTGAGCAAAGTAACCACAAGCG
	CDS-HSFA1d-Rv	AGGATTTTGCCTTGAGAGATCTAAGGT
HSFA1e	CDS-HSFA1e-Fw	ATGGGAACGGTTTGCGAATCTGTAGCG
	CDS-HSFA1e-Rv	TTTTCTGAGAGCATCTGATGTGAG
HSFA2	CDS-HSFA2-Fw	ATGGAAGAACTGAAAGTGGAAATGGAG
	CDS-HSFA2-Rv	AGGTTCCGAACCAAGAAAACCCATT
HSFA3	CDS-HSFA3-Fw	AGTCAGCAAAGAGGAAAAGAGGTTC
	CDS-HSFA3-Rv	GAATTAACCATTTTTTTGTTTACAC
HSFA4a	CDS-HSFA4a-Fw	ATGGATGAGAATAATCATGGAGT
	CDS-HSFA4a-Rv	ACTTCTCTCTGAAGAAGTCAGATG
HSFA4c	CDS-HSFA4c-Fw	ATGGATGAAAATAATGGAGGTTC
	CDS-HSFA4c-Rv	AGAAGCTTTCTCTGTAATGTTAT
	CDS-HSFA5-Fw	ATGAACGGCGCATTAGGTAAC

doi:10.6342/NTU202500611

HSFA5	CDS-HSFA5-Rv	TAAGGTCAGCTGCTCGATATTCTT
HSFA6a	CDS-HSFA6a-Fw	ATGGATTATAACCTTCCAATTCCA
	CDS-HSFA6a-Rv	TATAAAATGTTCCACTAAATCACAC
HSFA6b	CDS-HSFA6b-Fw	ATGGATCCTTCATTTAGGTTCATTA
	CDS-HSFA6b-Rv	ATTAGTGTGTGAACTAGAACCCAAA
HSFA7a	CDS-HSFA7a-Fw	ATGATGAACCCGTTTCTCCC
	CDS-HSFA7a-Rv	GGAGGTGGAAGCCAAACTCTCA
HSFA7b	CDS-HSFA7a-Fw	ATGGACCCGTCGTCAAGCTCCAGA
	CDS-HSFA7a-Rv	ATCTTGCTTCACATTCGCCTCTT
HSFA8	CDS-HSFA7b-Rv	ATCTTGCTTCACATTCGCCTCTT
	CDS-HSFA8-Rv	TTCATTTGAAGCCAGCAATTCCATC
HSFA9	CDS-HSFA9-Fw	ATGACGGCAATTCCAAACGTC
	CDS-HSFA9-Rv	CTCTATCTCTATCCTCCCATT
HSFB1	CDS-HSFB1-Fw	ATGACGGCTGTGACGGCGGCGCAA
	CDS-HSFB1-Rv	GTTGCAGACTTTGCTGCTTTTCCAC
HSFB2a	CDS-HSFB2a-Fw	ATGAATTCGCCGCCGGTTGA
	CDS-HSFB2a-Rv	ATTACAAACTCTCTGATTGGTTCG
HSFB2b	CDS-HSFB2b-Fw	ATGCCGGGGGAACAAACCGGAGAAA
	CDS-HSFB2b-Rv	TTTTCCGAGTTCAAGCCACGACCCA
HSFC1	CDS-HSFC1-Fw	ATGGAGGACGACAATAGTAACA
	CDS-HSFC1-Rv	GAATTAACCATTTTTTTGTTTACAC
RT-PCR		
	RT-HDA5-Fw	TTTTAGCCTTAACCAATCCGGT

doi:10.6342/NTU202500611

HDA5	RT-HDA5-Rv	CCTGAGGTAACGGGTTTTGA
qRT-PCR		
HSFA1d	q-HSFA1d-Fw	GTTTGGAAACCACCGGAGTTCG
	q-HSFA1d-Rv	GGTCAACCTTCCTGAAACCATAGG
HSFA2	q-HSFA2-Fw	GCAGCGTTGGATGTGAAAGTGG
	q-HSFA2-Rv	TTGGCTGTCCCAATCCAAAGGC
HSFA3	q-HSFA3-Fw	AAGAGACGACATGGAGCATGGG
	q-HSFA3-Rv	GCATCGGTGTTGCTGAAACTCG
HSFA7a	q-HSFA7a-Fw	ACCACCACCACAACCAATGGAG
	q-HSFA7a-Rv	TCTTGGTCAGAAATGGAGGTGGAG
HSFA7b	q-HSFA7b-Fw	ATGGAGGGATTGCAGGAAGCAG
	q-HSFA7b-Rv	TGGATCACCAACCATCTCGAACG
HSFB2b	q-HSFB2b-Fw	TGTTCGTCAGCTCAATACTTACGG
	q-HSFB2b-Rv	GCCGTTGAATATCCCGAAGCAG
HSP17.4	q-HSP17.4-Fw	ATGTCTCTAGTTCCGAGCTTT
	q-HSP17.4-Rv	CTTGAACACATGCGCTTCA
HSP18.2	q-HSP18.2-Fw	ACAAACGCAAGAGTGGATTGGA
	q-HSP18.2-Rv	GCTCCTCTCTCCGCTAATCTGC
HSP21	q-HSP21-Fw	TGGACGTCTCTCCTTTCGGATTGT
	q-HSP21-Rv	TGCACGAATCTCTGACACTCCACT
HSP22	q-HSP22-Fw	ATTCTGGAGACAGTTCAAGCTACCT
	q-HSP22-Rv	TTCAGGAGATAGTTTCGTGAGGTTA
	q-HSP70-B-Fw	GTACGTCGCCTTCACTGATAC

doi:10.6342/NTU202500611

HSP70-B	q-HSP70-B-Rv	GAGAACTTCCTTCCGATGAGAC
HSP101	q-HSP101-Fw	ACAACACTCTGTCTCTCGCCTCAT
	q-HSP101-Rv	CTGCCTTGCCCGTCTGTCAATC
APX2	q-APX2-Fw	ACCCTATCAAGGAGCTGTTCCC
	q-APX2-Rv	CCAGGATGAAATGGAATCTCTGGTC
HDA5	q-HDA5-Fw	AGATAGTGCTGGCGTTAGAGG
	q-HDA5-Rv	CGGAGGTCCTTGAATTTGTTTG
HDA6	q-HDA6-Fw	AAGTGGTGATCGGTTGGGTT
	q-HDA6-Rv	AGACGATGGAGGATTCACGT
HDA18	q-HDA18-Fw	GGAGAACTGGAGGCAAGGAG
	q-HDA18-Rv	CCAACTCGGCTTCTTGACCT
PP2A	q-PP2A-Fw	CCTGCGGTAATAACTGCATCT
	q-PP2A-Rv	CTTCACTTAGCTCCACCAAGCA
ChIP-qPCR		
HSP18.2	ChIP-HSP18.2-Fw	TATGTGTTCTAAAGACTCCA
	ChIP-HSP18.2-Rv	GTTAGAGGATGAAGAGAGAA
HSP22	ChIP-TSS-HSP22-Fw	CACAACAAACTTATCCAACG
	ChIP-TSS-HSP22-Rv	GGTAGAGTTTTGCAGAGAGA
	ChIP-400-HSP22-Fw	ACCAAAATCTCCATGACAAG
	ChIP-400-HSP22-Rv	GTGGTCCTGCCTTTACTTTTGG
	ChIP-3k-HSP22-Fw	CGTTGGACTTGGCCTTAGAT
	ChIP-3k-HSP22-Rv	TGACTGCTCCCTGATTCTTG
	ChIP-138-HSP101-Fw	ACATCTACCTGTCGGATCAA

doi:10.6342/NTU202500611

HSP101	ChIP-138-HSP101-Rv	TCTGGAAAGATAGAGAACTA
	ChIP-3.2k-HSP101-Fw	CTCTCAAAAAGTGTACCTCCA
	ChIP-3.2k-HSP101-Rv	GAGCTCCAAGAAAAGGCCAT
PP2A	q-PP2A-Fw	CCTGCGGTAATAACTGCATCT
	q-PP2A-Rv	CTTCACTTAGCTCCACCAAGCA

doi:10.6342/NTU202500611

Figures

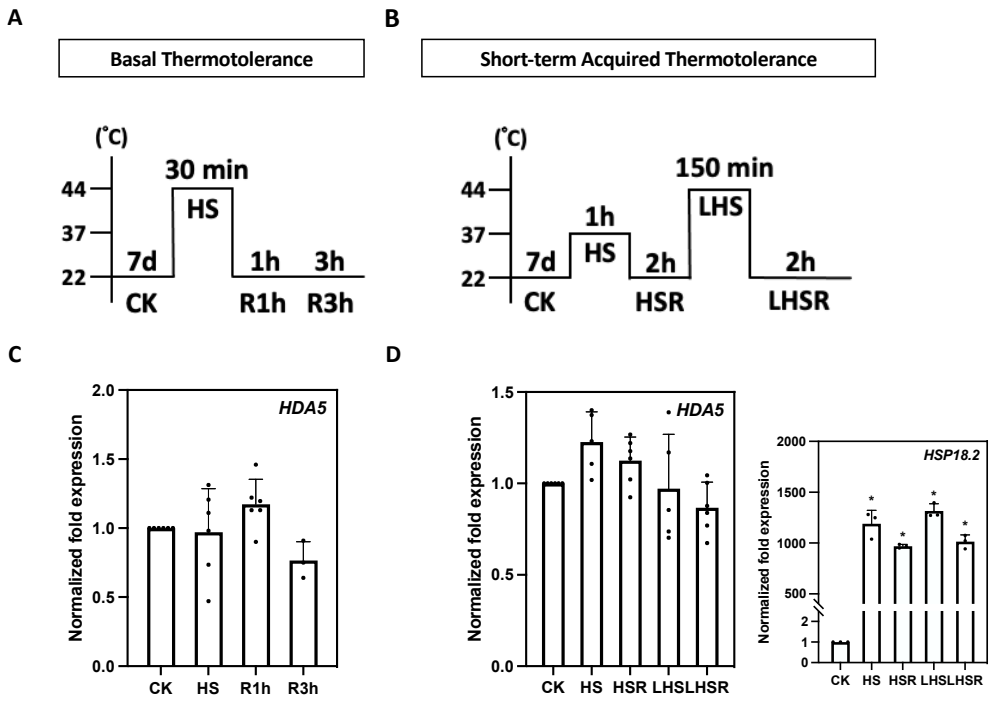

Figure 1. Transcriptional expressions of *HDA5* in response to heat stresses.

7-day-old Col-0 seedlings were treated with or without (control; CK) acute/moderate high temperature. Pictogram illustrated the schemes for (A) basal thermotolerance, (B) acquired thermotolerance treatments and recovery time. (C and D) Expression levels of HDA5 were analyzed. *HSP18.2* was used as a HS-responsive reference gene for short-term acquired thermotolerance test. Data are represented as mean ± SD of 3 independent experiments (N=3). *PP2A* was used as reference gene. All data were normalized to the *PP2A*. * indicated significance at $p < 0.05$ (Student's *t* test) compared to the CK.

doi:10.6342/NTU202500611

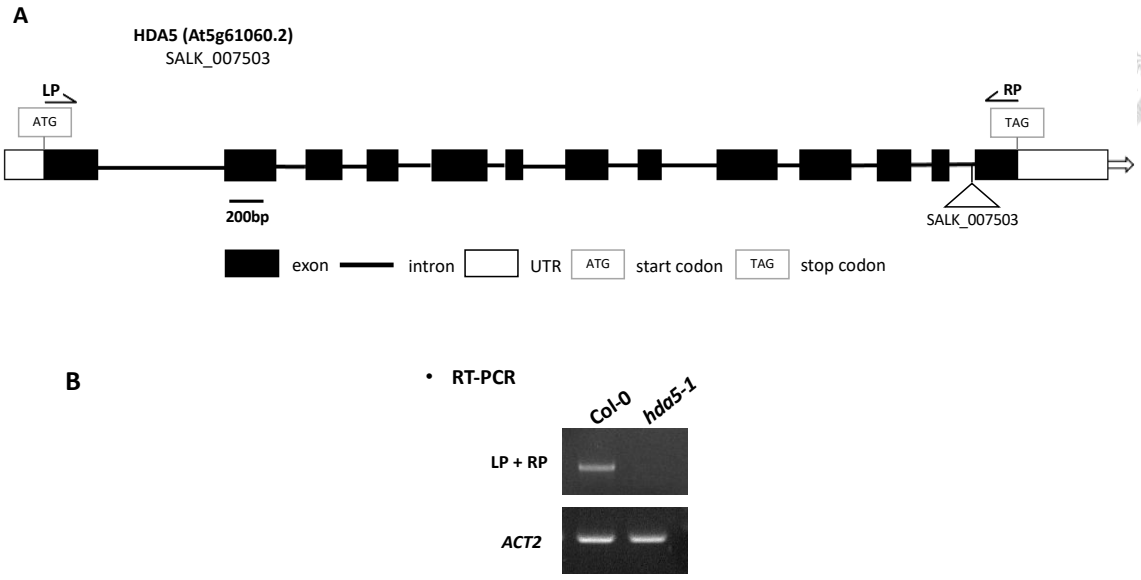

Figure 2. Characterization of *hda5* T-DNA insertion line.

The hollow triangle represents the T-DNA insertion site in *hda5-1* (SALK_007503). Black arrows represent the left primer (LP) and right primer (RP) used to amplify the full coding sequence region for the RT-PCR. (B) RT-PCR results indicated that *hda5-1* is a knock-out line. 32 cycles were used for amplifying target gene (LP x RP). *ACT2* was used as reference gene.

doi:10.6342/NTU202500611

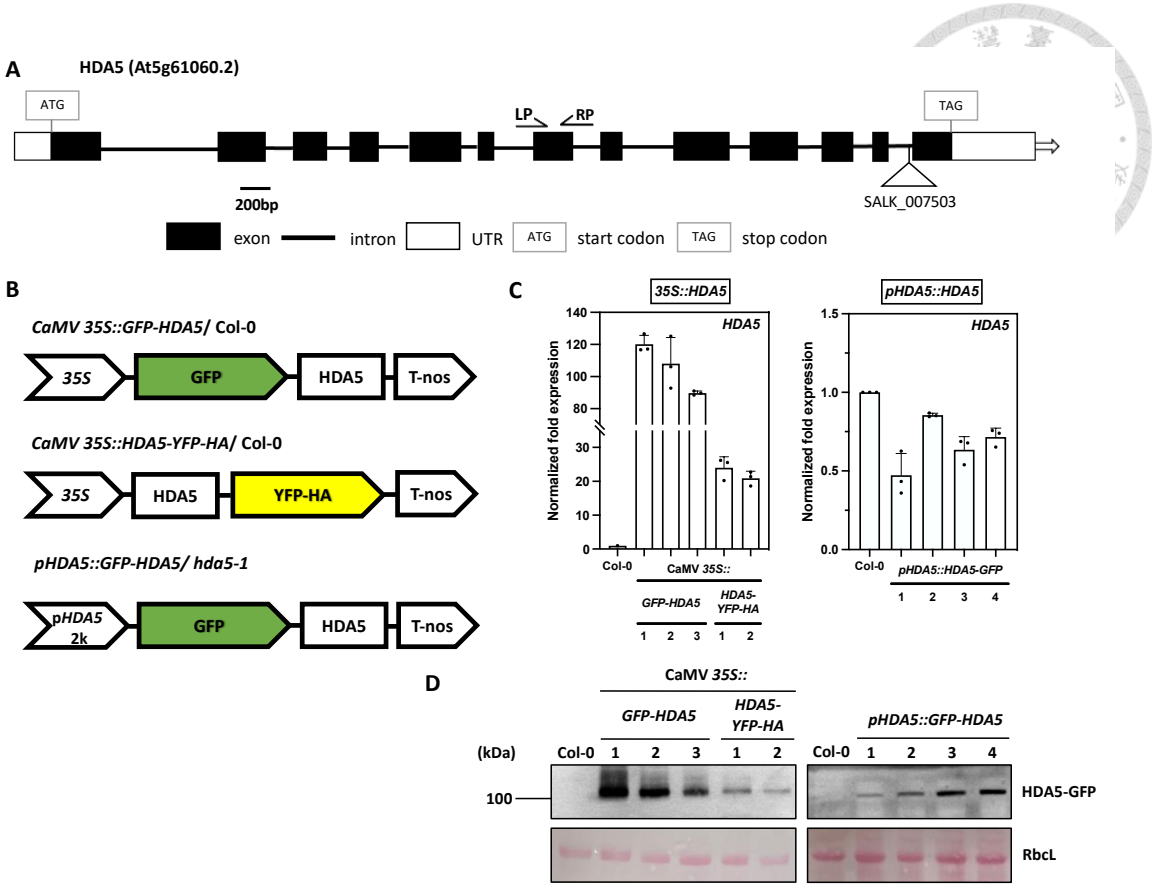

Figure 3. Characterization of the pCaMV *35S*/ *HDA5* Native Promoter-Driven *HDA5* Transgenic Lines.

The hollow triangle represents the T-DNA insertion site in *hda5-1* (SALK_007503). Black arrows represent the left primer (LP) and right primer (RP) used to amplify the full coding sequence region for the qPCR amplicon. (A) Plasmid construction of CaMV-driven pK7WGF2 and pEG101 with full-length *HDA5* CDS inserted. For GFP-tag (pK7WGF2) and YFP-HA-tag (pEG101) were designed at the N-terminus and C-terminus of *HDA5*, respectively. The Col-0 background was used for CaMV- driven

doi:10.6342/NTU202500611

HDA5 transgenic lines. A 2kb region of *HDA5* promoter was used for *HDA*5 native promoter- driven line. The GFP-tag (pK7WGF2) were designed at the N-terminus of full-length *HDA5* CDS. *hda5-1* (SALK_007503) was used as background for HDA5 native promoter-driven line. (B and C) 7-day-old Col-0 seedlings were used for qRT-PCR analysis and western blotting. The expression levels of *HDA5* were analyzed in both *35S::HDA5* and *pHDA5::HDA5* transgenic lines. *PP2A* was used as reference gene. All data were normalized to *PP2A.* Data are represented as mean ± SD of 3 independent replicates (N=3). For western blotting, GFP antibody was used to detect the GFP-HDA5 and HDA5-YFP signals. The MW of GFP-tagged HDA5 is approximately 100 kDa. Ponceau S stained RBcL was used as loading control.

doi:10.6342/NTU202500611

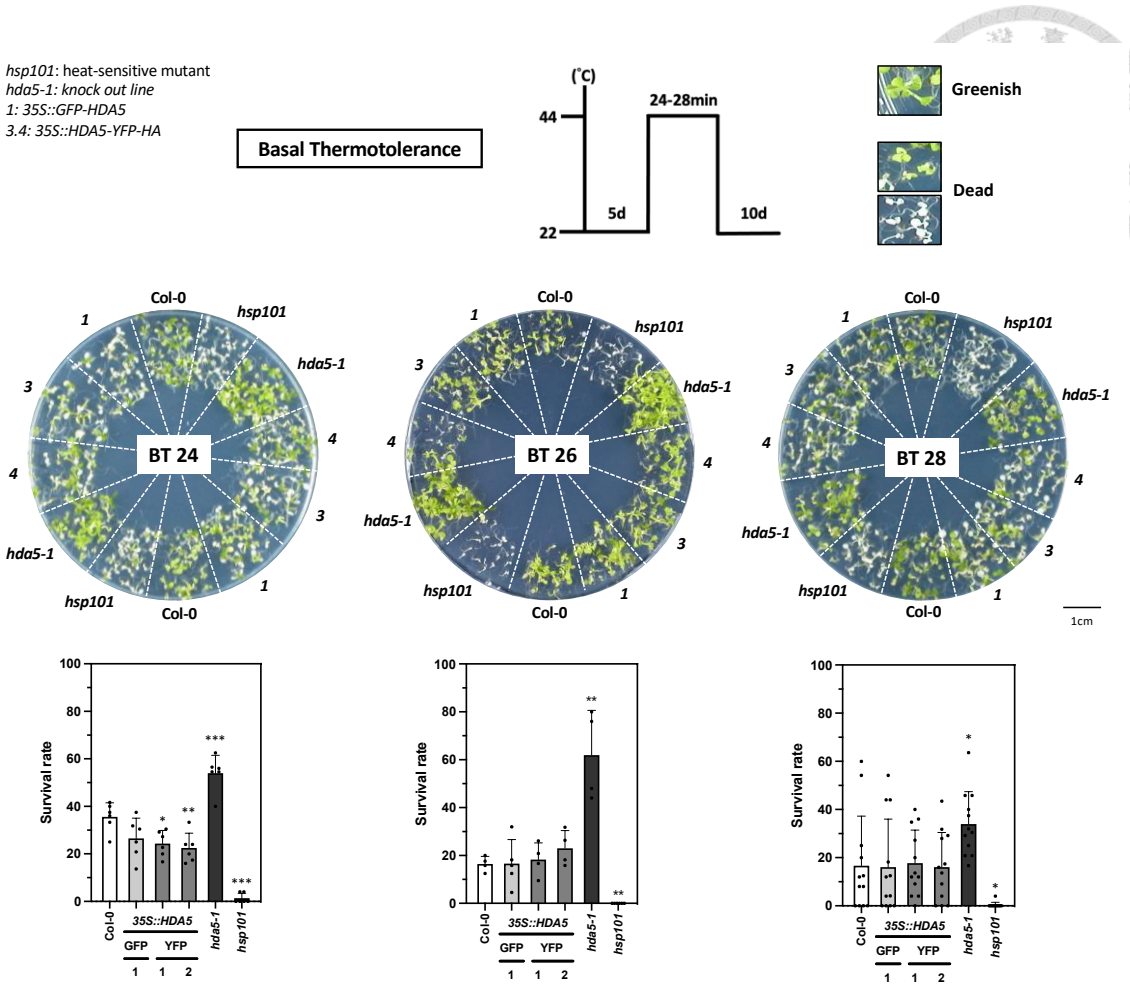

Figure 4. Basal thermotolerance tests of *hda5-1* and *35S::HDA5* transgenic lines.

The schematic representation of basal thermotolerance (BT) treatments is shown at the top. Five-day-old seedlings were subjected to BT with varying durations of lethal temperature exposure. The enlarged figure illustrates the survival or death status after 10 days of recovery. Photos (A) and survival rates (B) were captured and measured 10 days post-treatment, respectively. Data are represented as mean ± SD of three independent biological replicates (N=9, n=25). Asterisks indicate statistically significant difference (Student's *t*-test: *$p \leq 0.05$; **$p \leq 0.01$; ***$p \leq 0.001$) compared to Col-0.

doi:10.6342/NTU202500611

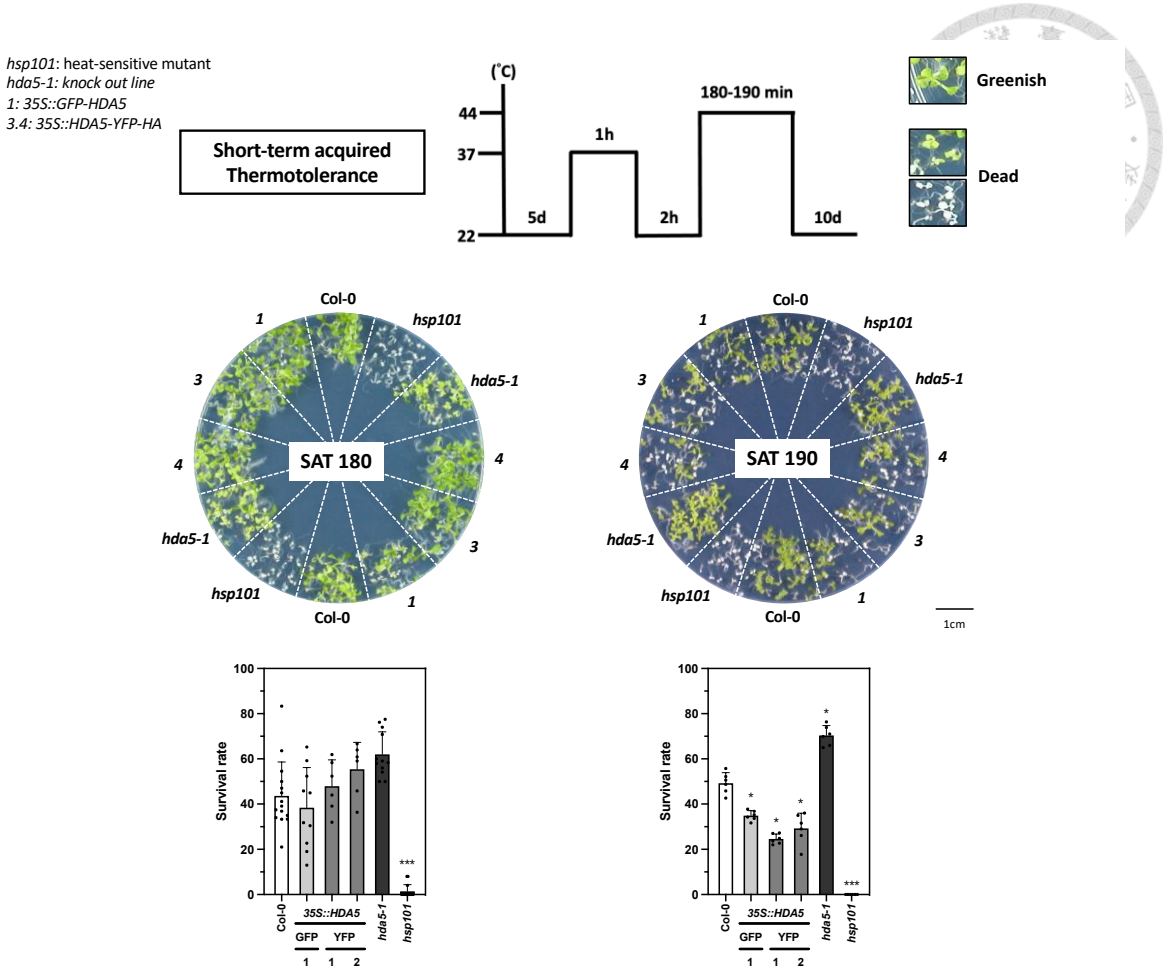

Figure 5. Short-term acquired thermotolerance tests of *hda5-1* and *35S::HDA5* transgenic lines.

The schematic representation of short-term acquired thermotolerance (SAT) treatments is shown at the top. Five-day-old seedlings were subjected to SAT with varying durations of lethal temperature exposure. The enlarged figure illustrates the survival or death status after 10 days of recovery. Photos (A) and survival rates (B) were captured and measured 10 days post-treatment, respectively. Data are represented as mean ± SD of three independent biological replicates (N=9, n=25). Asterisks indicate statistically significant difference (Student's *t*-test: *$p \leq 0.05$; **$p \leq 0.01$; ***$p \leq 0.001$) compared to Col-0.

doi:10.6342/NTU202500611

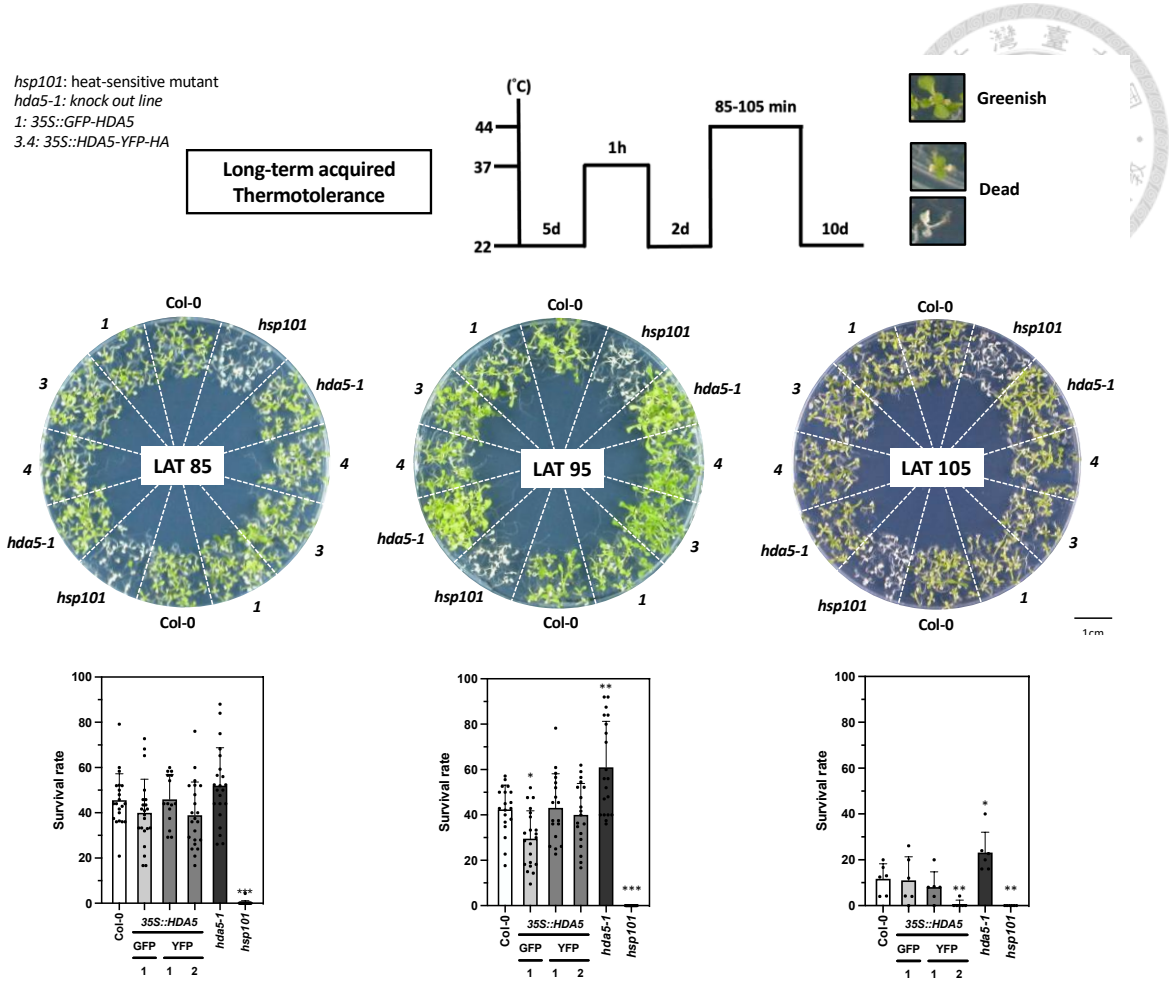

Figure 6. Long-term acquired thermotolerance tests of *hda5-1* and *35S::HDA5* transgenic lines.

The schematic representation of long-term acquired thermotolerance (LAT) treatments is shown at the top. Five-day-old seedlings were subjected to LAT with varying durations of lethal temperature exposure. The enlarged figure illustrates the survival or death status after 10 days of recovery. Photos (A) and survival rates (B) were captured and measured 10 days post-treatment, respectively. Data are represented as mean ± SD of three independent biological replicates (N=9, n=25). Asterisks indicate statistically significant difference (Student's *t*-test: *$p \leq 0.05$; **$p \leq 0.01$; ***$p \leq 0.001$) compared to Col-0.

doi:10.6342/NTU202500611

A

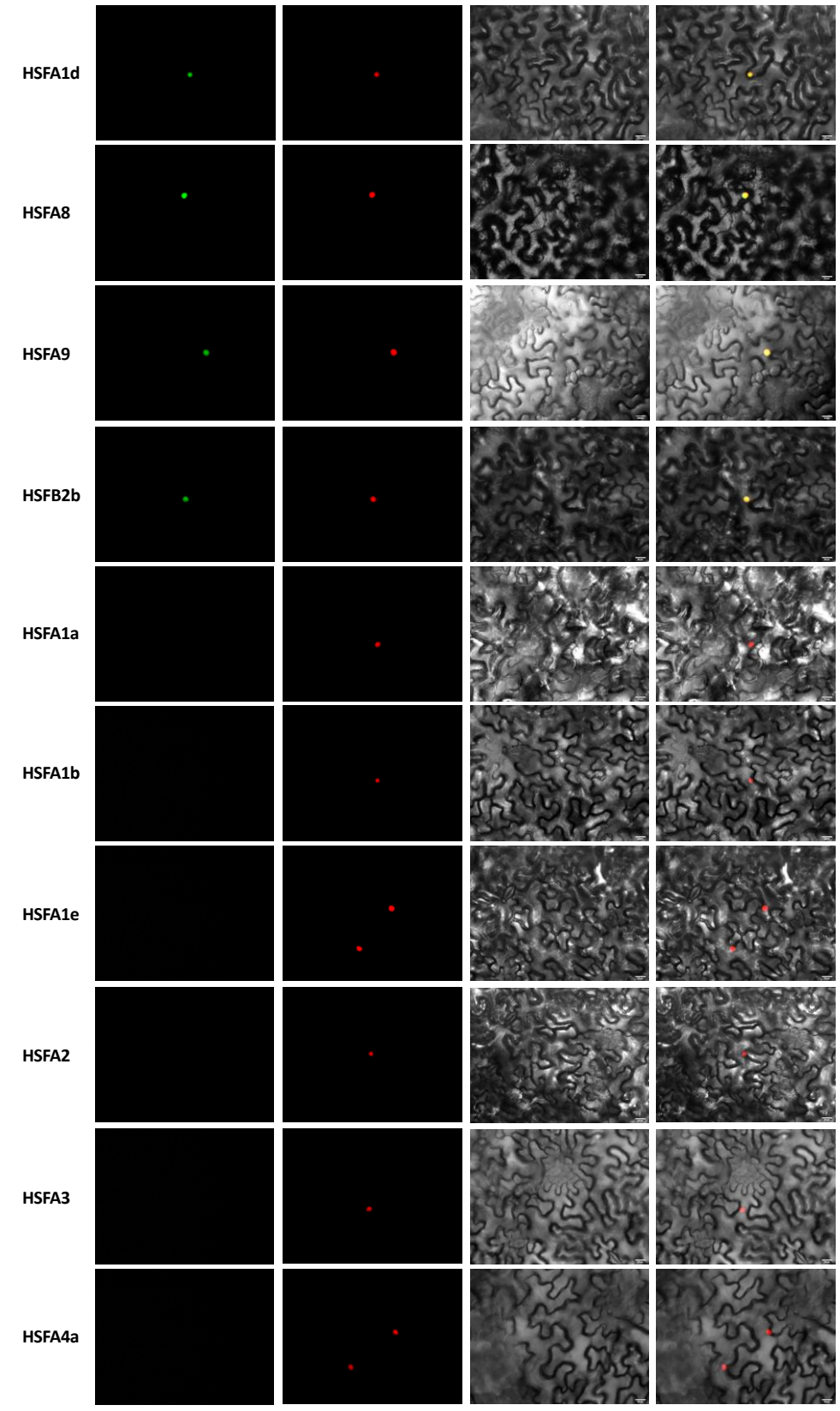

doi:10.6342/NTU202500611

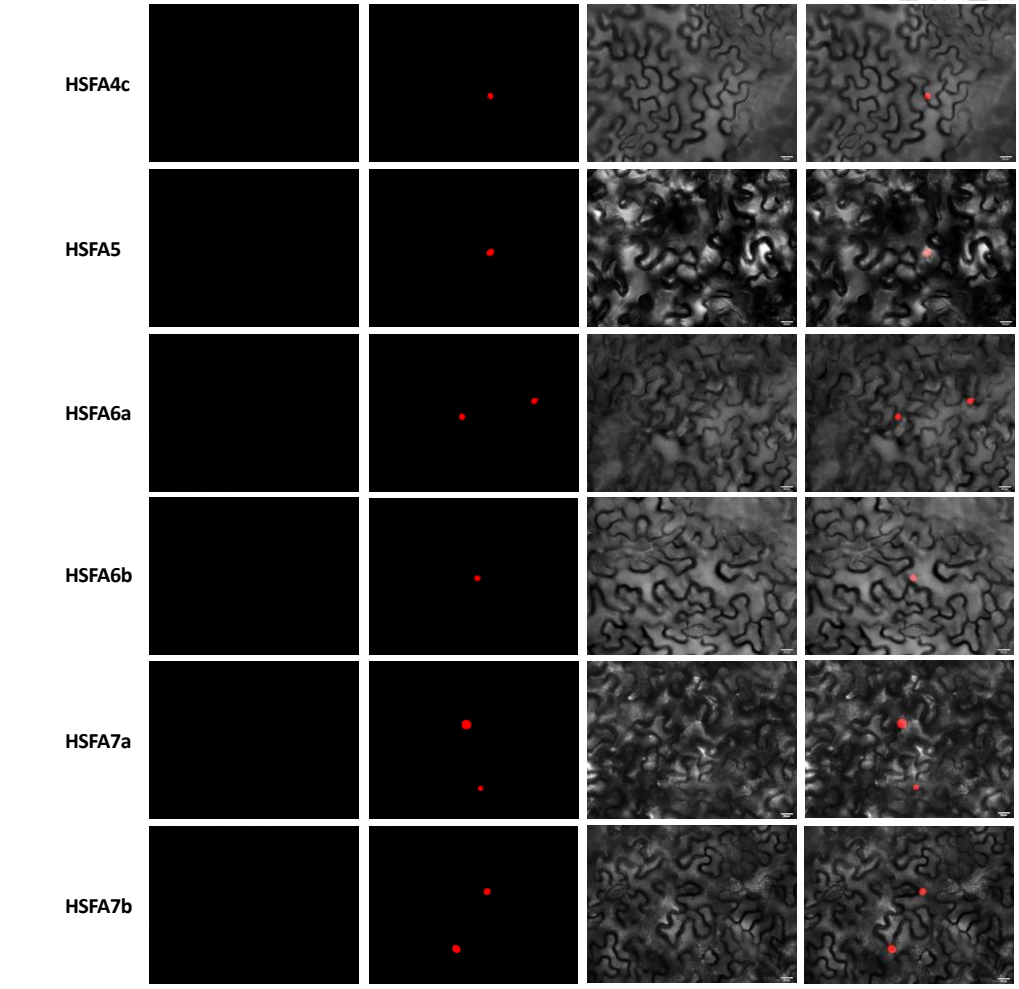

B

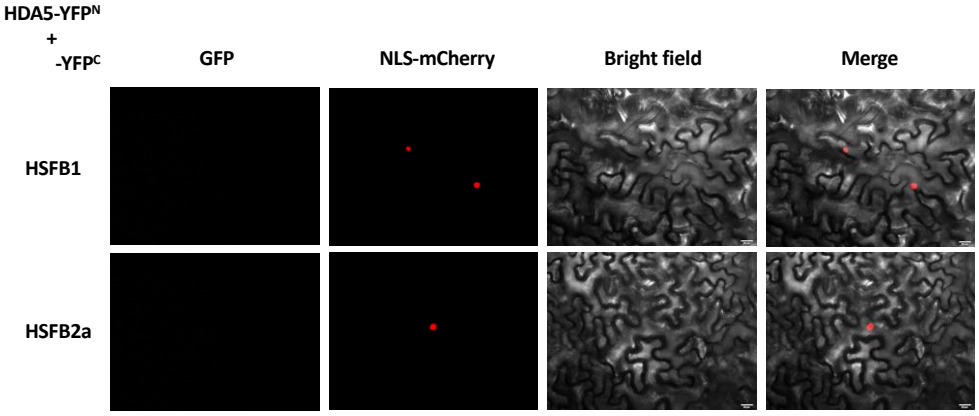

C

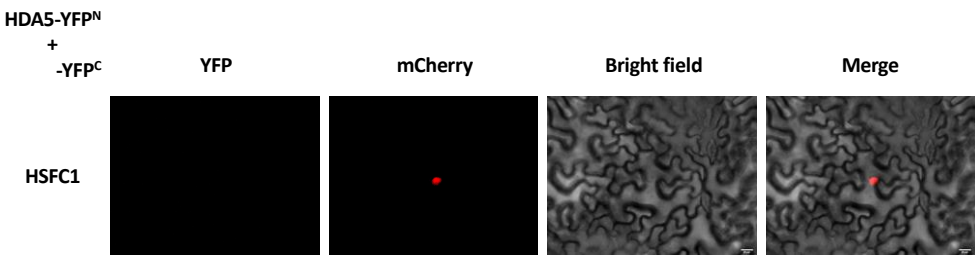

doi:10.6342/NTU202500611

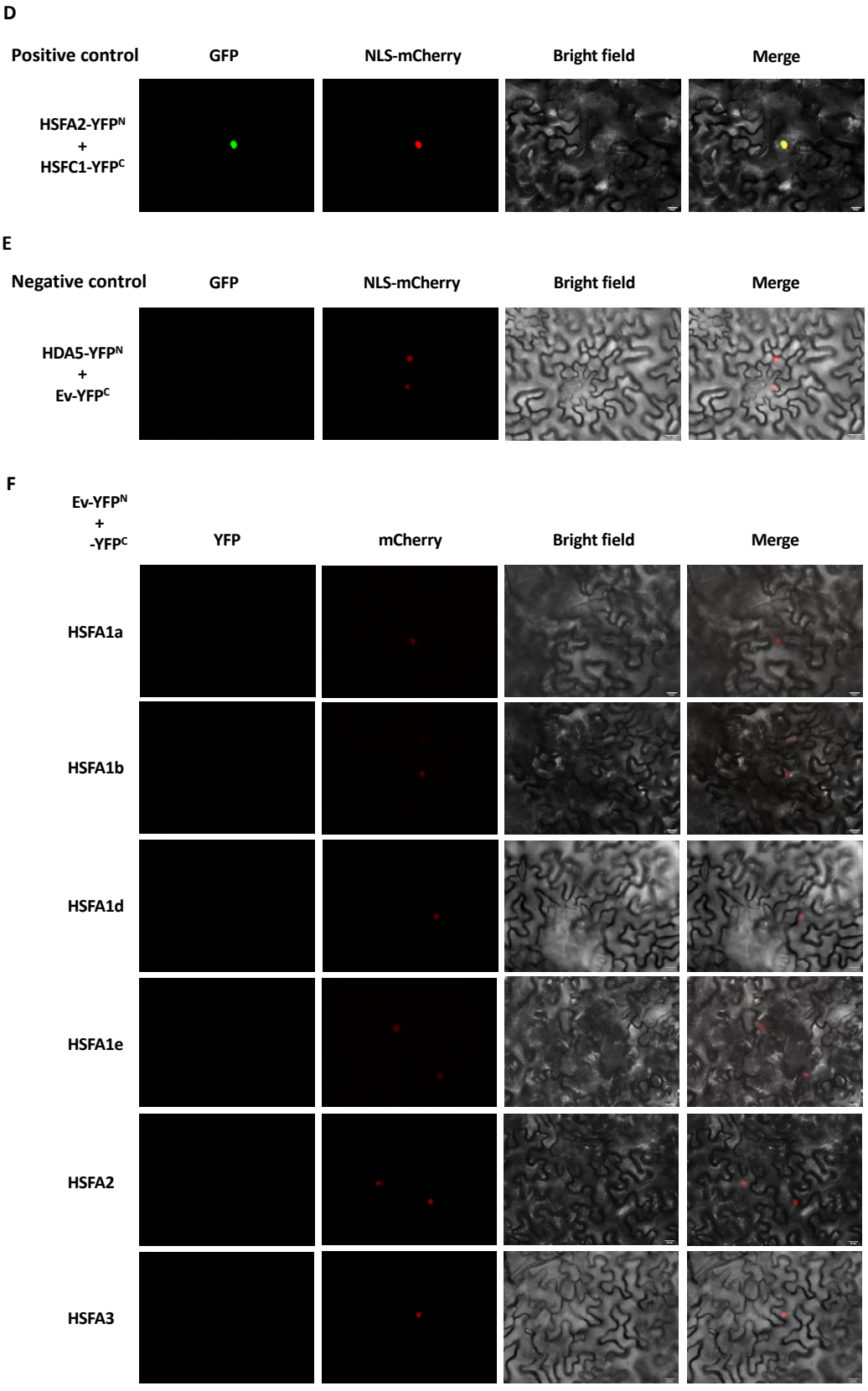

doi:10.6342/NTU202500611

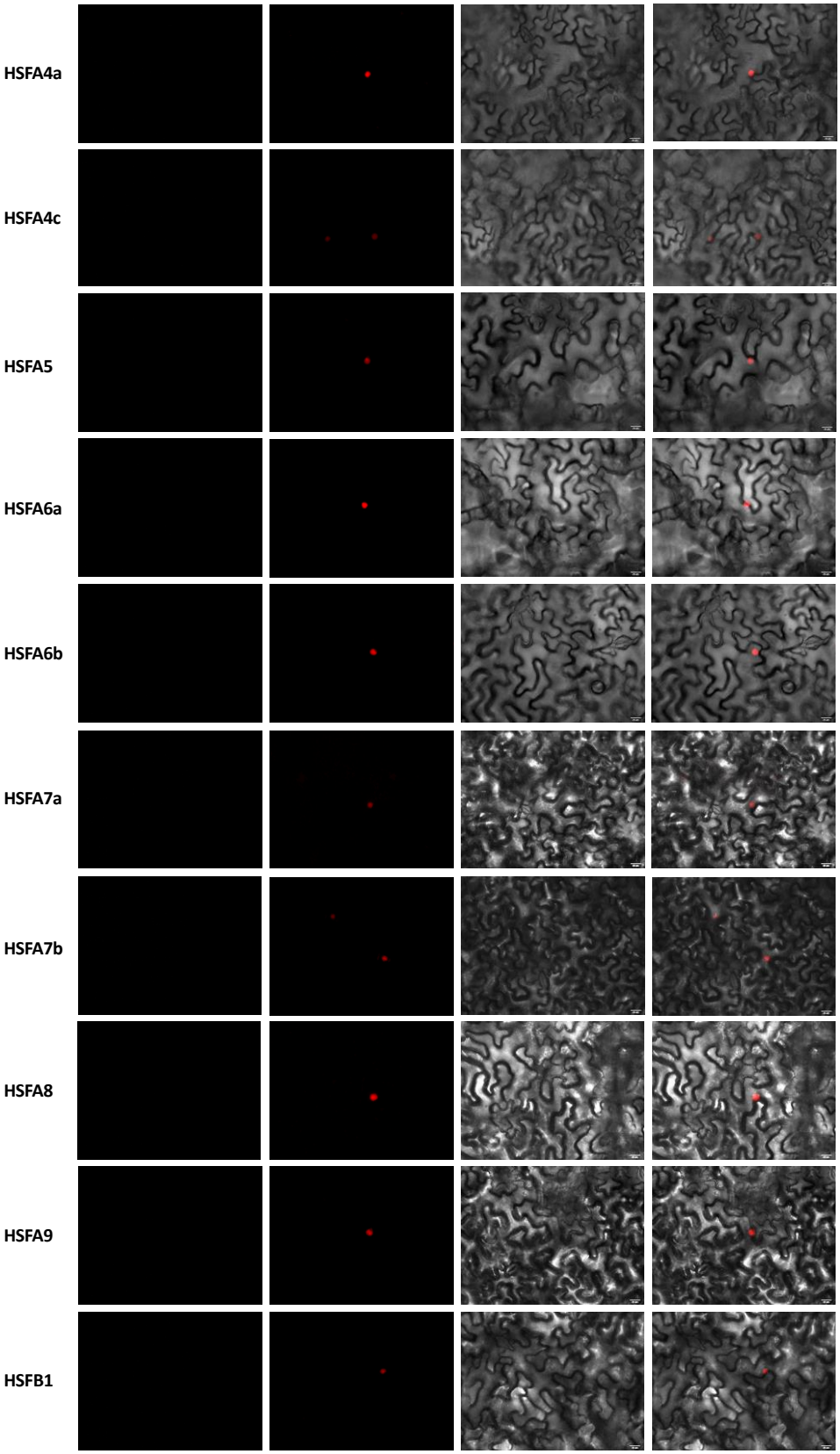

doi:10.6342/NTU202500611

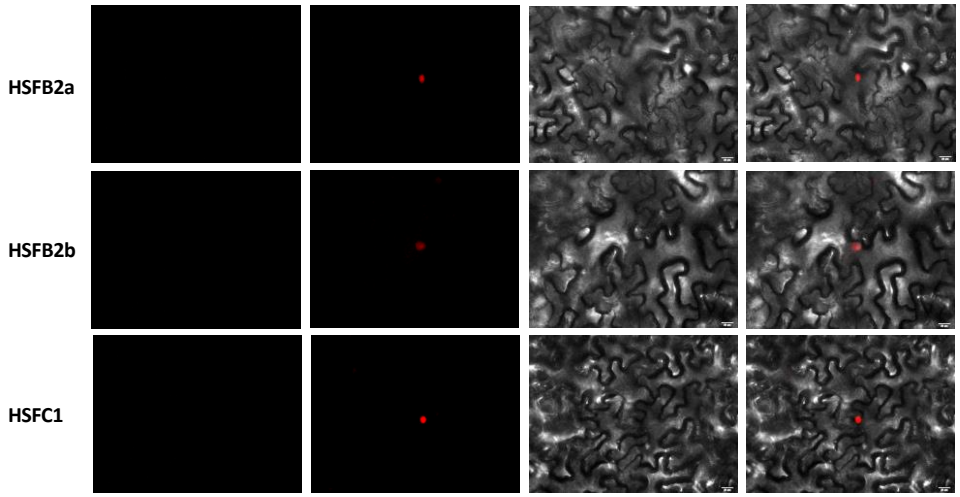

Figure 7. BiFC screening of interactions between HDA5-Y^N and HSF's-Y^C.

Agro-infiltration were performed to transient expressing HDA5-Y^N, HSF's-Y^C (excepting HSFB3 and HSFB4), Ev-Y^N and Ev-Y^C in *N. benthamiana*. (A to C) HSFA, HSFB, HSFC classes were analyzed with HDA5, as indicated. (D) HSFA2-Y^N +HSFC1-Y^C were used as positive control. HDA5-Y^N + Ev-Y^C (E) and Ev-Y^N + HSF's-Y^C (F) were analyzed as negative control. NLS-mCherry was used as nuclear marker. Scale bar = 20 μm.

doi:10.6342/NTU202500611

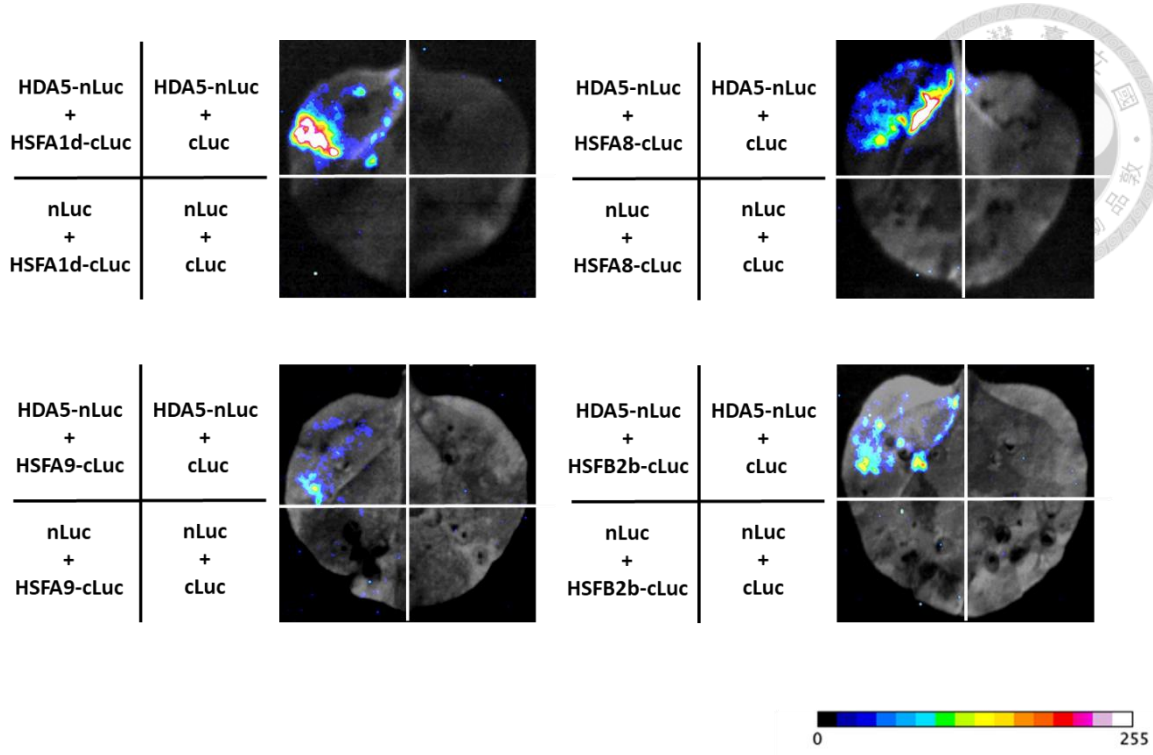

Figure 8. Split-luciferase complementation (Split-LUC) imaging assay of HDA5 interacts with HSFA1d, HSFA8, HSFA9 and HSFB2b.

Agro-infiltration were performed to transient expressing HDA5-nLuc, HSFA1d-, HSFA8-, HSFA9, HSFB2b-cLuc, Ev-nLuc and Ev-cLuc in *N. benthamiana*. Tobacco leaves were separated into four sections. Each section was subjected with different combination of agrobacterium. Luminescence signals were detected via imaging system (iBright 750, Invitrogen). ImageJ was used for colored the strength of luminescence signals. Scale of 16 colors is represented as from weak (black) to strong (white) luminescence signals.

doi:10.6342/NTU202500611

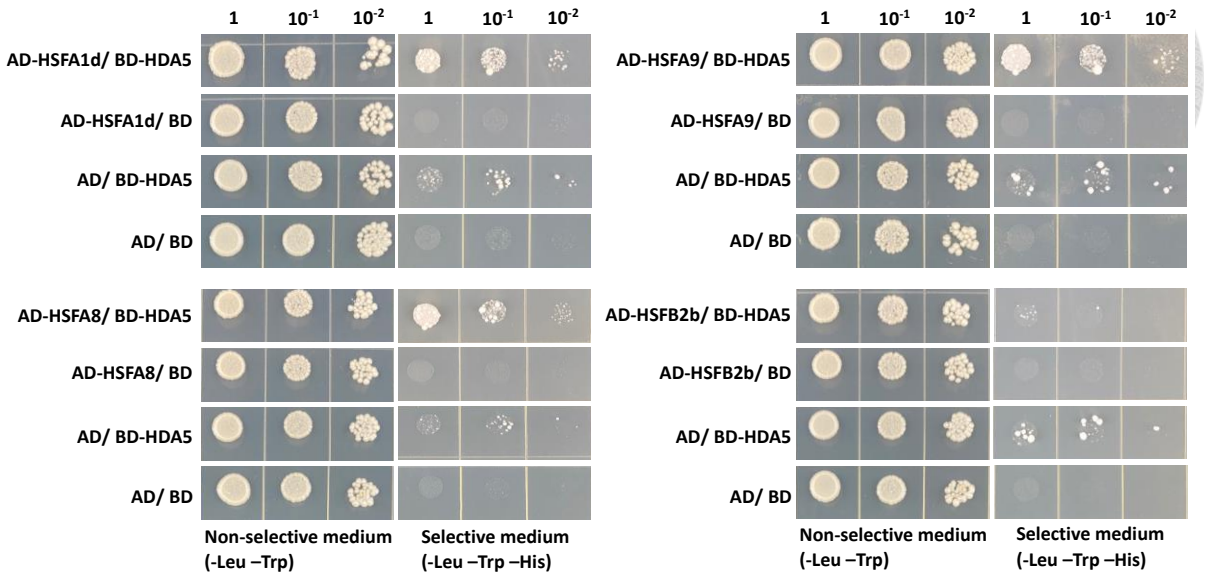

Figure 9. Yeast two hybrid assay of HDA5 interacts with HSFA1d, HSFA8, HSFA9 and HSFB2b.

HDA5-BD (*Y187*), HSFA1d-, HSFA8, HSFA9, HSFB2b-AD (*AH109*), Ev-AD and Ev-BD were mating with different combinations as described and the concentration were adjusted to an OD of 0.6 (1x) and diluted to 10^{-1} and 10^{-2}, following by incubate on non-selective medium (-Leu –Trp) and selective medium (-Leu -Trp –His) for 7 days.

doi:10.6342/NTU202500611

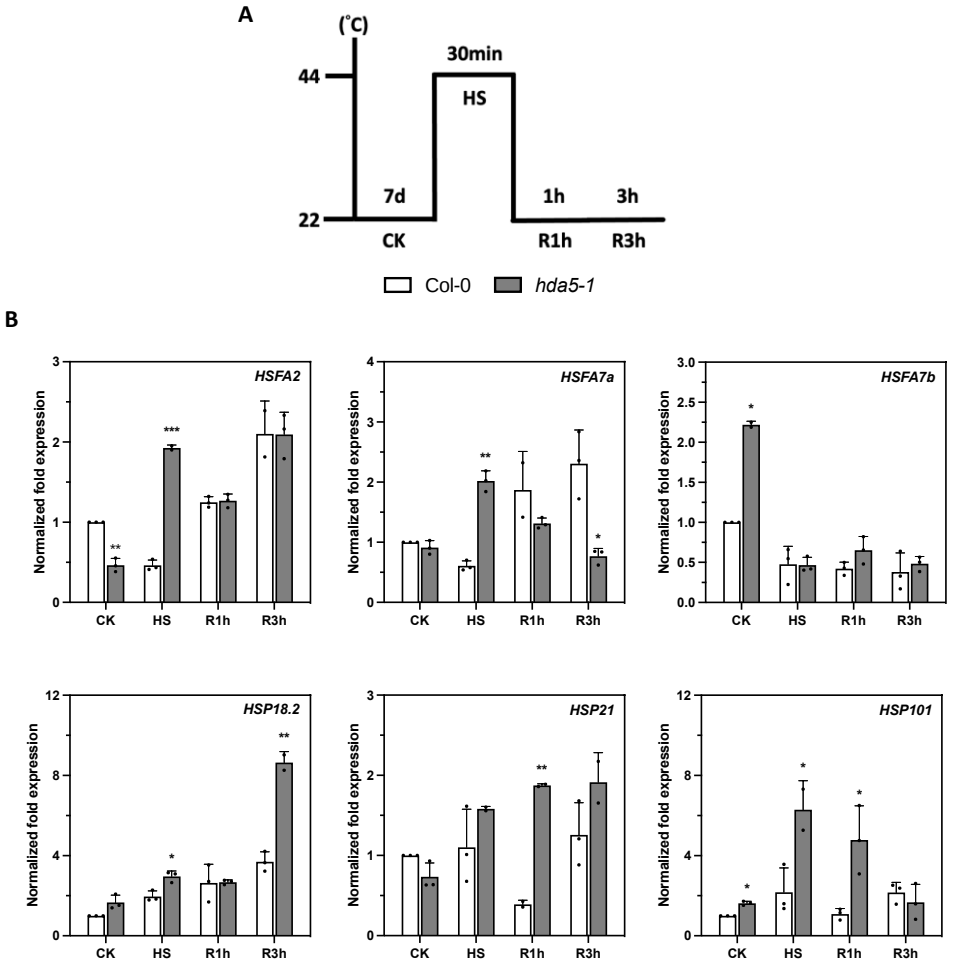

Figure 10. The expression levels of HS-responsive genes in *Col-0* and *hda5-1* upon lethal heat stress.

(A) Schematic representation of the experimental setup. (B) The expression levels of *HSFA2*, *HSFA7a*, *HSFA7b*, *HSP18.2*, *HSP21* and *HSP101*. Data was represented as mean ± SD of 3 independent experiments (N=3). Asterisks indicate statistically significant difference (Student's *t*-test: *$p \leq 0.05$; **$p \leq 0.01$; ***$p \leq 0.001$) compared to Col-0 CK. *PP2A* was used as loading control. All data were normalized to *PP2A*.

doi:10.6342/NTU202500611

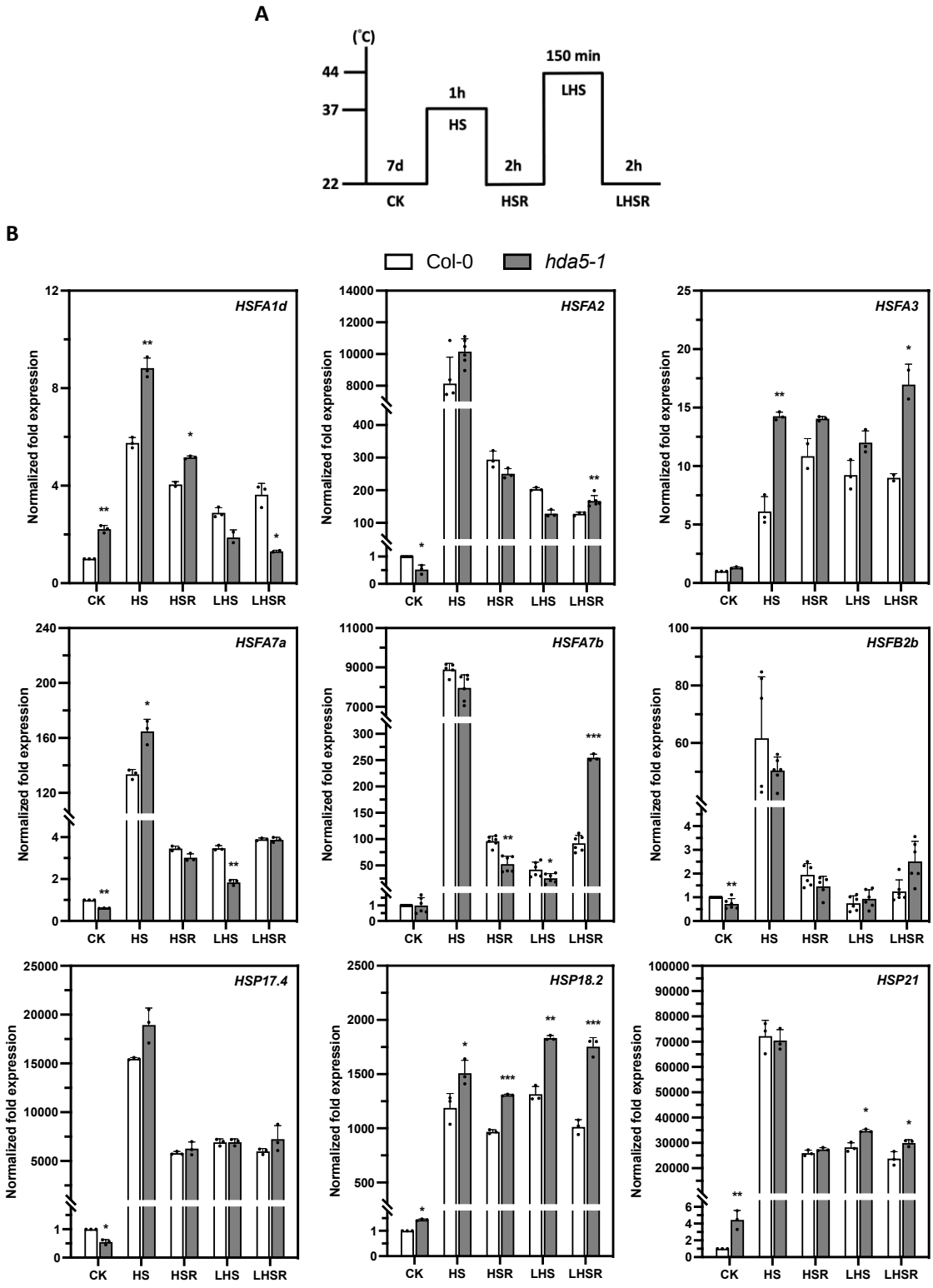

doi:10.6342/NTU202500611

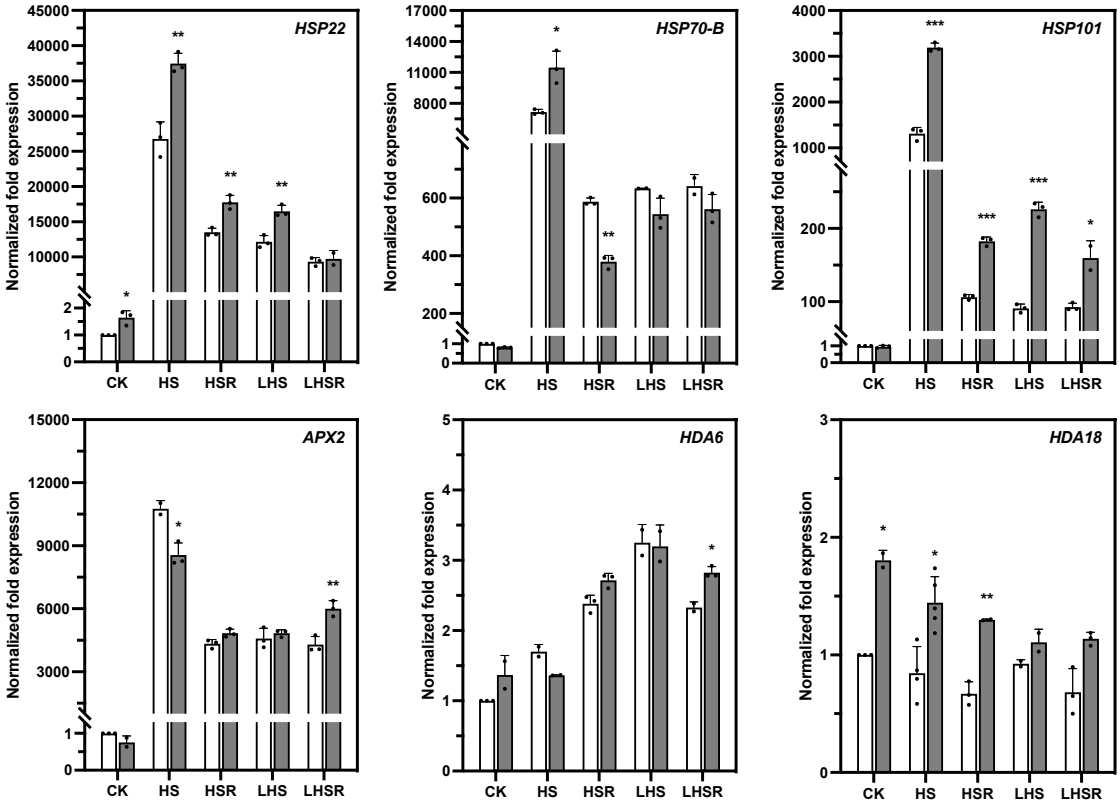

Figure 11. The expression levels of HSFs, HSPs, *APX2, HDA6* and *HDA18* in Col-0 and *hda5-1* in response to short-term AT treatment.

(A) Schematic representation of the experimental setup. (B) The expression levels of *HSFA1d*, *HSFA2*, *HSFA3*, *HSFA7a*, *HSFA7b*, *HSFB2b*, *HSP17.4*, *HSP18.2*, *HSP21*, *HSP22*, *HSP70-B*, *HSP101*, *APX2*, *HDA6* and *HDA18*. Data was represented as mean ± SD of 3 independent experiments (N=3). Asterisks indicate statistically significant difference (Student's *t*-test: *$p \leq 0.05$; **$p \leq 0.01$; ***$p \leq 0.001$) compared to Col-0 CK. *PP2A* was used as loading control. All data were normalized to *PP2A*.

doi:10.6342/NTU202500611

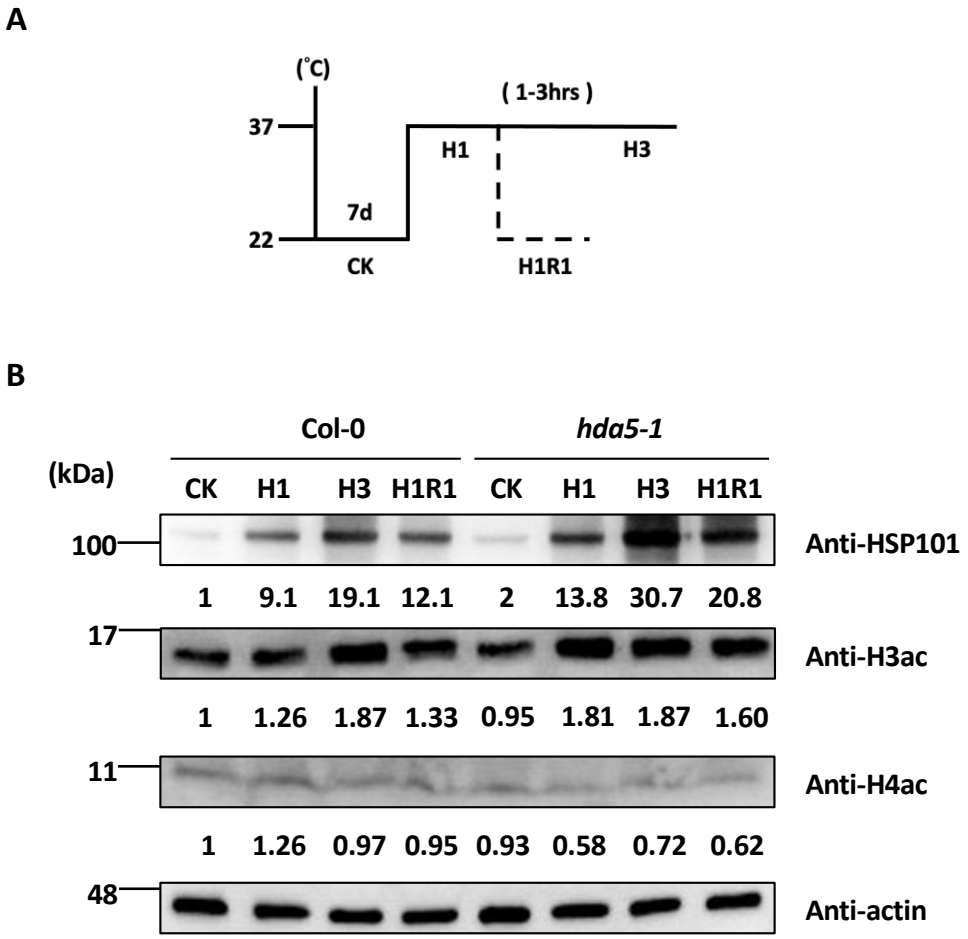

Figure 12. Protein abundance assay in Col-0 and *hda5-1*.

100 seven-day-old Col-0 and *hda5-1* seedlings were subjected to moderate high-temperature treatment. Control groups (CK) were left untreated. (A) Schematic of Heat Treatment. The dotted line indicates the H1R1 samples treated at 37°C for 1 hr, followed by a 1-hr recovery in the growth chamber. (B) Protein levels in Col-0 and *hda5-1* under heat stress were assessed via Western blot. Antibodies used included anti-HSP101, anti-H3Ac, and anti-H4Ac to detect the protein abundance. The molecular mass (MS) of HSP101, acetyl-H3, acetyl-H4, and actin are 101 kDa, 15 kDa, 10 kDa, and 45 kDa,

doi:10.6342/NTU202500611

respectively. ImageJ software was used for quantifying protein bands. Actin was used as the loading control.

doi:10.6342/NTU202500611

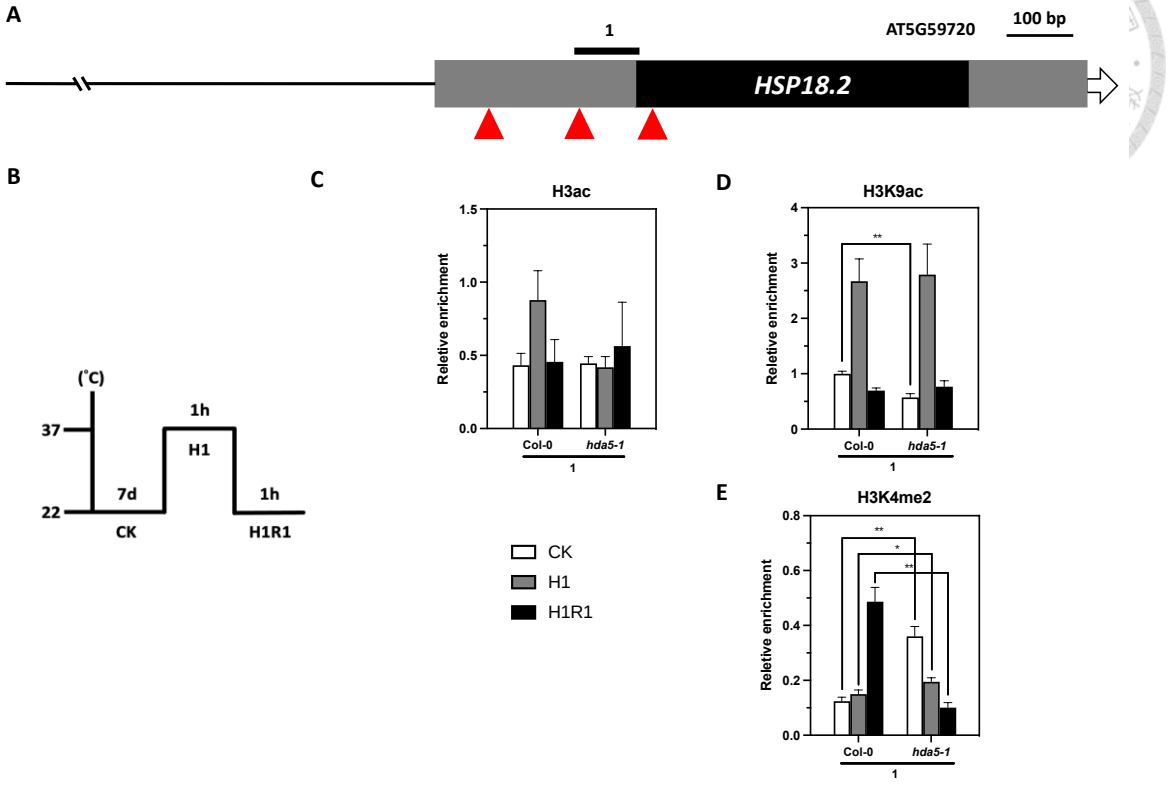

Figure 13. The levels of H3ac, H3K9ac and H3K4me2 on *HSP18.2* loci in Col-0 and *hda5-1* upon heat stress.

(A) The schematic diagram of *HSP18.2* genomic section. The gray rectangle, red triangle and black line are represented as 5' or 3' UTR, the site of heat shock element (HSE) and amplicons of q-PCR, respectively. (B) (A) Schematic of Heat Treatment. (C) ChIP-qPCR analysis of the levels of H3ac, H3K9ac and H3K4me2 on *HSP18.2* loci. The levels of H3ac were normalized to *ACT2*. The levels of H3K9ac and H3K4me2 were normalized to H3. Asterisks indicate statistically significant difference (Student's *t*-test: $*p \leq 0.05$; $**p \leq 0.01$; $***p \leq 0.001$) compared to Col-0.

doi:10.6342/NTU202500611

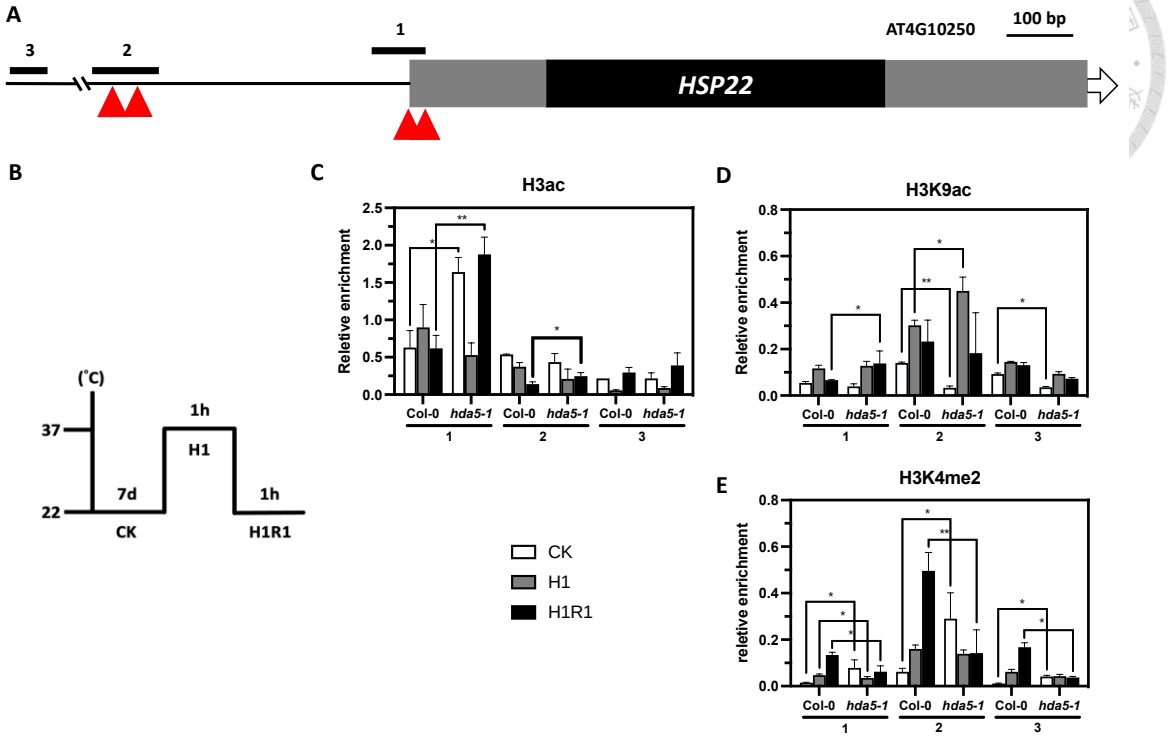

Figure 14. The levels of H3ac, H3K9ac and H3K4me2 on *HSP22* loci in Col-0 and *hda5-1* upon heat stress.

(A) The schematic diagram of *HSP22* genomic section. The gray rectangle, red triangle and black line are represented as 5' or 3' UTR, the site of heat shock element (HSE) and amplicons of q-PCR, respectively. (B) (A) Schematic of Heat Treatment. (C) ChIP-qPCR analysis of the levels of H3ac, H3K9ac and H3K4me2 on *HSP22* loci. The levels of H3ac were normalized to *ACT2*. The levels of H3K9ac and H3K4me2 were normalized to H3. Asterisks indicate statistically significant difference (Student's *t*-test: $*p \leq 0.05$; $**p \leq 0.01$; $***p \leq 0.001$) compared to Col-0.

doi:10.6342/NTU202500611

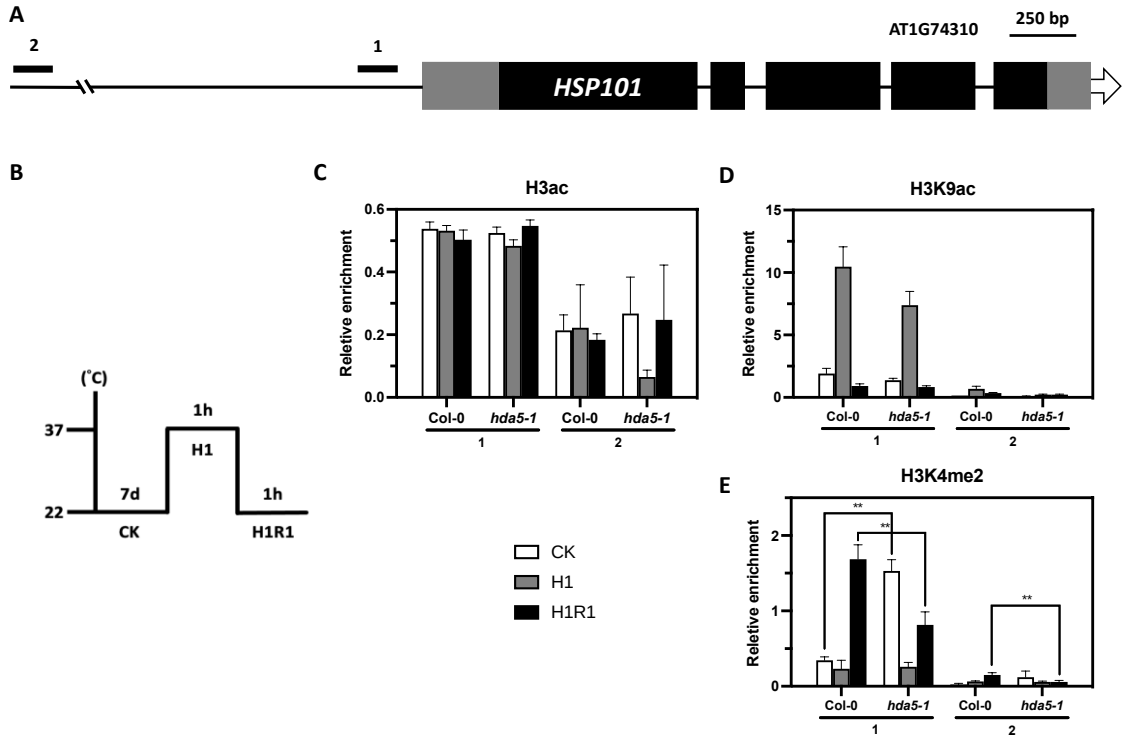

Figure 15. The levels of H3ac, H3K9ac and H3K4me2 on *HSP101* loci in Col-0 and *hda5-1* upon heat stress.

(A) The schematic diagram of *HSP101* genomic section. The gray rectangle, red triangle and black line are represented as 5' or 3' UTR, the site of heat shock element (HSE) and amplicons of q-PCR, respectively. (B) (A) Schematic of Heat Treatment. (C) ChIP-qPCR analysis of the levels of H3ac, H3K9ac and H3K4me2 on *HSP101* loci. The levels of H3ac were normalized to *ACT2*. The levels of H3K9ac and H3K4me2 were normalized to H3. Asterisks indicate statistically significant difference (Student's *t*-test: $*p \leq 0.05$; $**p \leq 0.01$; $***p \leq 0.001$) compared to Col-0.

doi:10.6342/NTU202500611

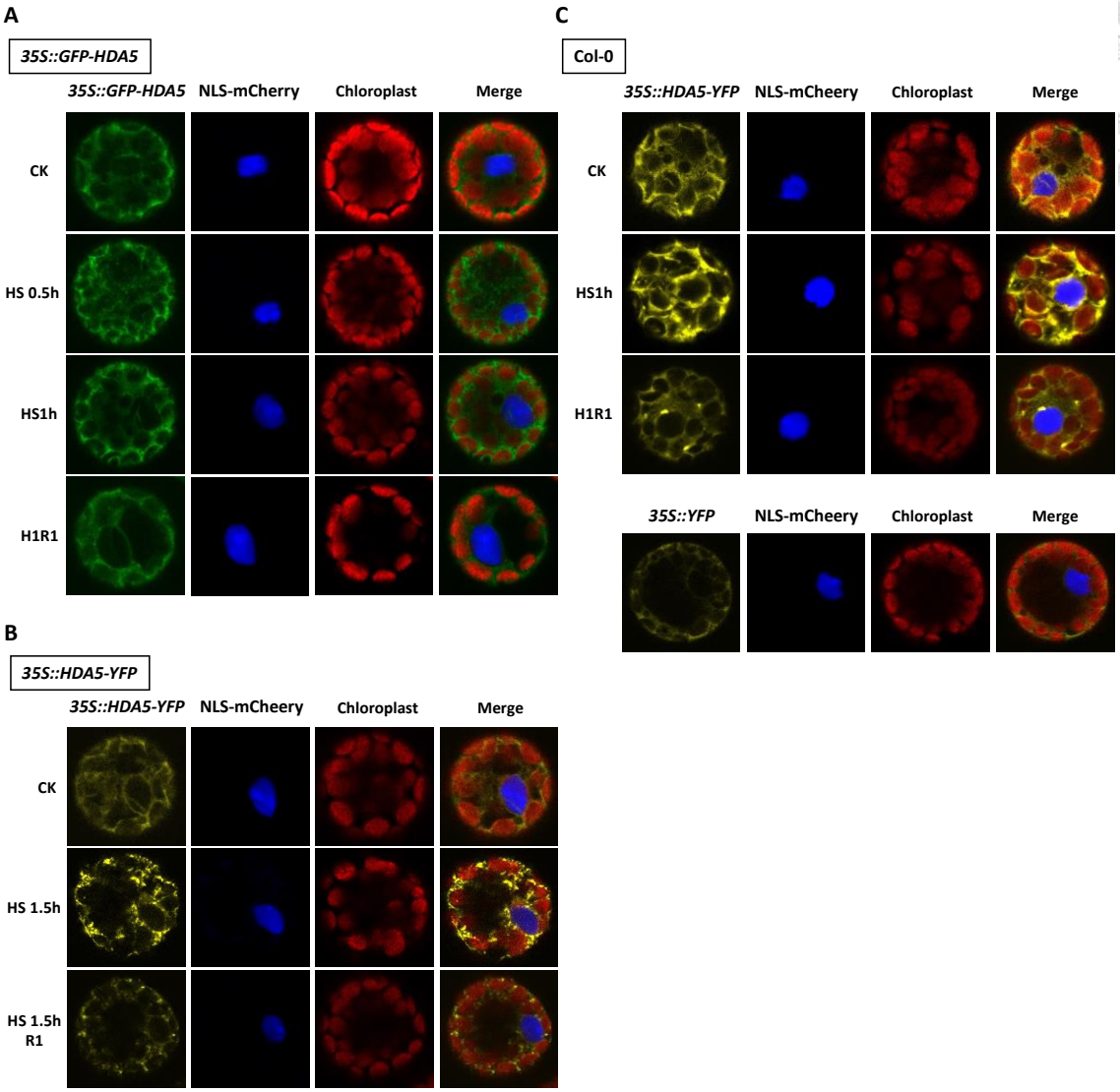

Figure 16. Subcellular localization of HDA5 upon heat stress.

35S::GFP-HDA5 (A), *35S::HDA5-YFP* (B) transgenic lines and Col-0 (C) was used for *Arabidopsis* mesophyll protoplasts extraction. GFP and YFP fluorescence was detected in GFP and YFP channel, respectively, using a confocal microscope. NLS-mCherry was used as a nuclear marker. The red signal was captured from the autofluorescence of

doi:10.6342/NTU202500611

chloroplasts. Samples were photographed immediately after being treated with or without heat stress.

doi:10.6342/NTU202500611

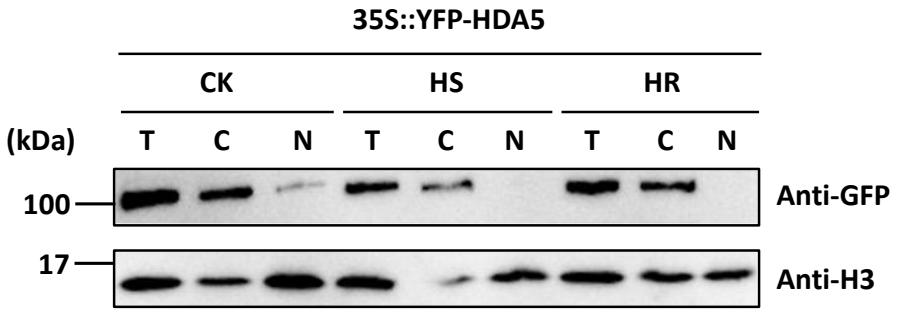

Figure 17. Nuclear-cytoplamic fractionation of HDA5 upon heat stress.

35S::YFP-HDA5 was used for nucleus fraction. Protein was extracted after treatment. GFP antibody was used for detected the HDA5-GFP signal. H3 antibody was used for nucleus control. T, total protein extract. C, cytosol extract. N, nucleus extract.

doi:10.6342/NTU202500611

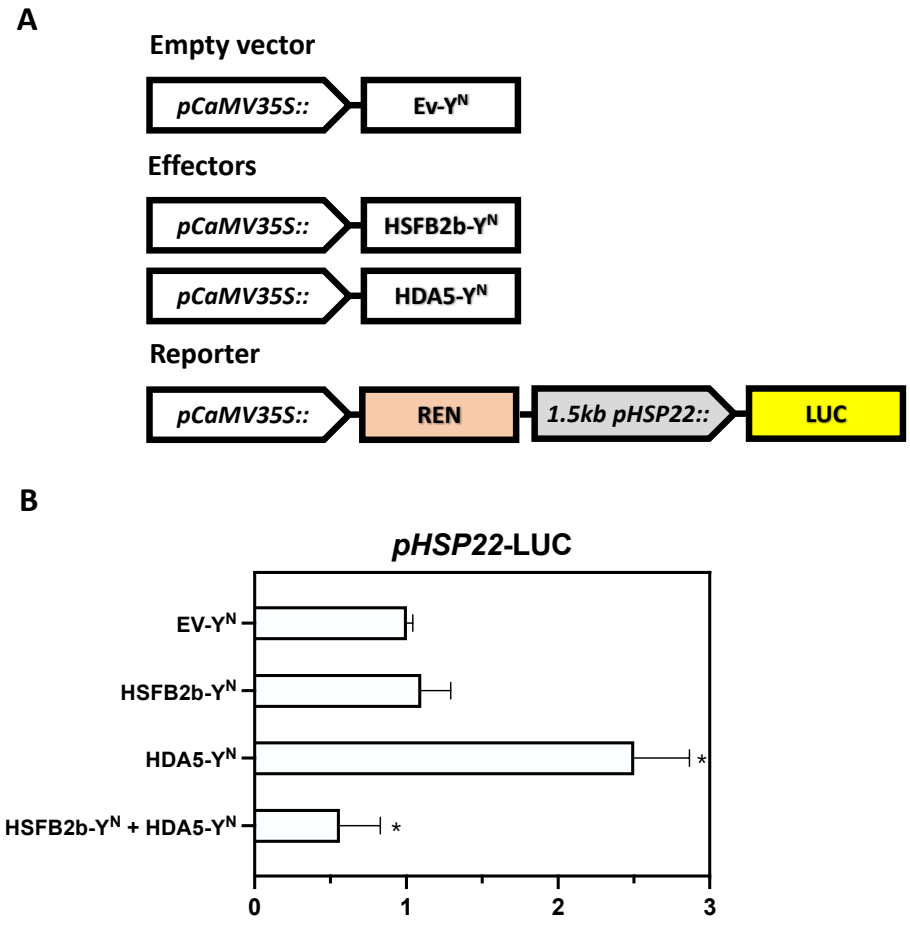

Figure 18. HDA5 and HSFB2b repressed the transcriptional activity of *HSP22*.

(A) The schematic representation of the effectors and reporter construction. For effectors, full-length *HSFB2b* and *HDA5* CDS were inserted in *pCaMV35S*::Y^N vector. For the reporter, REN and LUC were driven by the *pCaMV35S* and *1.5 kb pHSP22*, respectively. (B) The concentrations of agrobacterium were calculated as equal amount for each combination before infiltration. All data were normalized to REN. * indicates significance at $P < 0.05$ (Student's t-test).

doi:10.6342/NTU202500611

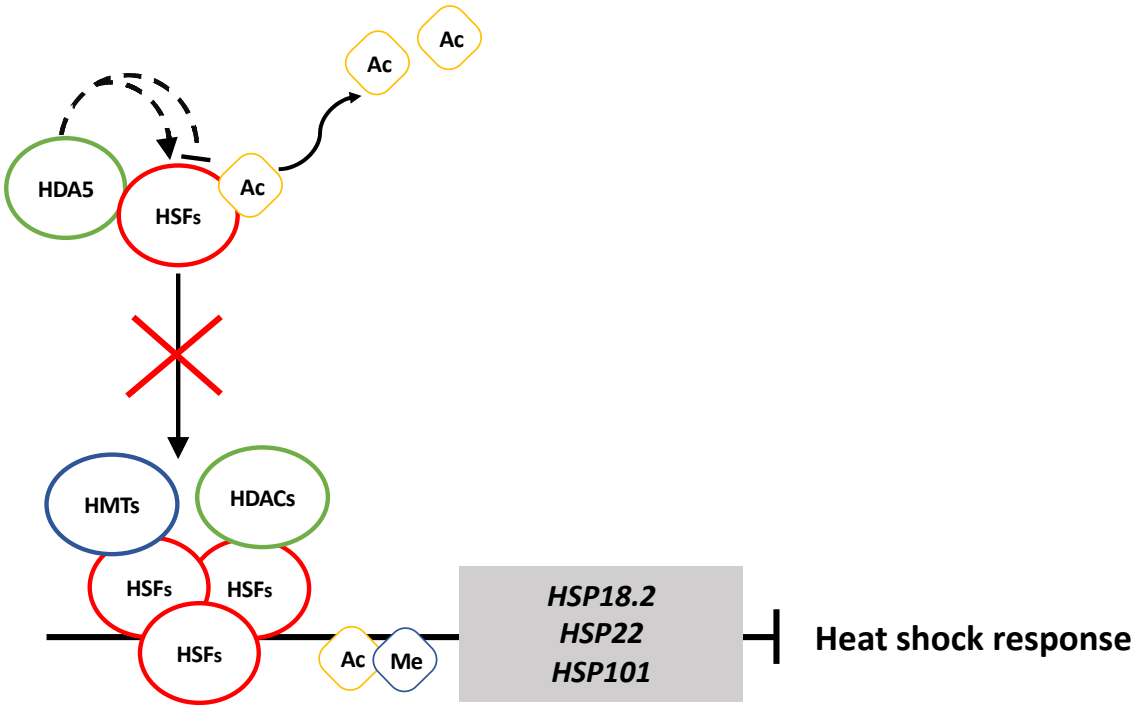

Figure 19. Illustration of HDA5 functions in HSR.

HDA5 may activate or inactivate HSFs, including HSFA1d, HSFA8, HSFA9, and HSFB2b, through deacetylation, thereby inhibiting HSF complex formation and repressing the HSR as well as three major HS-responsive genes: *HSP18.2*, *HSP22*, and *HSP101*. HDA5, histone deacetylase 5; HSFs, heat shock factors; HMTs, histone methyltransferases; Ac, acetylation; Me, methylation.

doi:10.6342/NTU202500611

Supplemental Figures

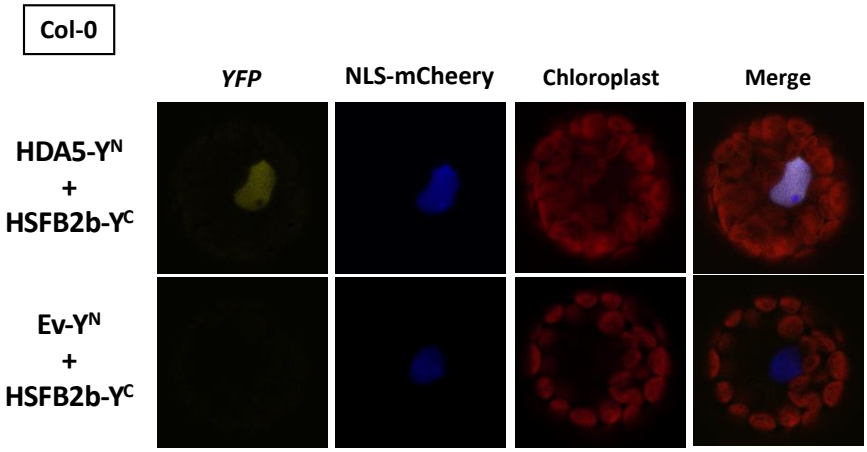

Supplemental Fig 1. BiFC interactions of HDA5-Y^N and HSFB2b-Y^C in *Arabidopsis* mesophyll protoplasts.

PEG-mediated method was performed to transfect the HDA5-Y^N and HSFB2b-Y^C plasmids into *Arabidopsis* (Col-0) mesophyll protoplasts. Yellow signal shown the reconstituted YFP fluorescence was detected in YFP channel via confocal microscope. NLS-mCheery was used as nuclear marker. The red signal represented as auto-fluorescence of chloroplast.

doi:10.6342/NTU202500611

References

Alinsug, M.V., Yu, C.W., and Wu, K. (2009). Phylogenetic analysis, subcellular localization, and expression patterns of RPD3/HDA1 family histone deacetylases in plants. BMC Plant Biology **9,** 37.

Andrási, N., Pettkó-Szandtner, A., and Szabados, L. (2020). Diversity of plant heat shock factors: regulation, interactions, and functions. Journal of Experimental Botany **72,** 1558-1575.

Bannister, AJ., and Kouzarides, T. (2011). Regulation of chromatin by histone modifications. Cell Research **21,** 381–395

Berger, S.L. (2002). Histone modifications in transcriptional regulation. Current Opinion in Genetics & Development **12,** 142-148.

Berger, S.L. (2007). The complex language of chromatin regulation during transcription. Nature **447,** 407–412.

Bernatavichute, Y.V., Zhang, X., Cokus, S., Pellegrini, M., and Jacobsen, S.E. (2008). Genome-wide association of histone H3 lysine nine methylation with CHG DNA methylation in *Arabidopsis thaliana*. PLoS One **39,** e3156.

Blum, A. (2005). Drought resistance, water-use efficiency, and yield potential—are they compatible, dissonant, or mutually exclusive? Australian Journal of Agricultural Research **56,** 1159-1168.

Bolger, A.M., Lohse, M., and Usadel, B. (2014). Trimmomatic: a flexible trimmer for Illumina sequence data. Bioinformatics **30,** 2114-2120.

Charng, Y.Y., Liu, H.C., Liu, N.Y., Chi, W.T., Wang, C.N., Chang, S.H., and Wang, T.T. (2007). A heat-inducible transcription factor, HsfA2, is required for extension of acquired thermotolerance in Arabidopsis. Plant Physiology **143,** 251-262.

Cheeseman, J.M. (1988). Mechanisms of salinity tolerance in plants. Plant Physiology **87,** 547-550.

Chen, C.Y., Tu, Y.T., Hsu, J.C., Hung, H.C., Liu, T.C., Lee, Y.H., Chou, C.C., Cheng, Y.S., and Wu, K. (2020). Structure of Arabidopsis HISTONE DEACETYLASE 15. Plant Physiology **184,** 1585-1600.

Cortijo, S., Charoensawan, V., Brestovitsky, A., Buning, R., Ravarani, C., Rhodes, D., van Noort, J., Jaeger, K.E., and Wigge, P.A. (2017). Transcriptional regulation of the ambient temperature response by H2A. Z nucleosomes and HSF1 transcription factors in Arabidopsis. Molecular Plant **10,** 1258-1273.

doi:10.6342/NTU202500611

de Ruijter, A.J., van Gennip, A.H., Caron, H.N., Kemp, S., and van Kuilenburg, A.B. (2003). Histone deacetylases (HDACs): characterization of the classical HDAC family. Biochemical Journal **15,** 737-749.

Demidchik, V. (2015). Mechanisms of oxidative stress in plants: from classical chemistry to cell biology. Environmental and Experimental Botany **109,** 212-228.

Du, J., Johnson, L.M., Jacobsen, S.E., and Patel, D.J. (2015). DNA methylation pathways and their crosstalk with histone methylation. Nature Reviews Molecular Cell Biology **16,** 519-532.

Fang, Y., and Xiong, L. (2015). General mechanisms of drought response and their application in drought resistance improvement in plants. Cellular and Molecular Life Sciences **72,** 673-689.

Fong, P., Tian, L., and Chen, Z. (2006). *Arabidopsis thaliana* histone deacetylase 1 (AtHD1) is localized in euchromatic regions and demonstrates histone deacetylase activity *in vitro*. Cell Research **16**, 479-488.

Friedrich, T., Oberkofler, V., Trindade, I., Altmann, S., Brzezinka, K., Lamke, J., Gorka, M., Kappel, C., Sokolowska, E., Skirycz, A., Graf, A., and Baurle, I. (2021). Heteromeric HSFA2/HSFA3 complexes drive transcriptional memory after heat stress in Arabidopsis. Nature Communications **12,** 3426.

Giesguth, M., Sahm, A., Simon, S., and Dietz, K.J. (2015). Redox-dependent translocation of the heat shock transcription factor AtHSFA8 from the cytosol to the nucleus in *Arabidopsis thaliana*. FEBS letters **589,** 718-725.

Gregoretti, I.V., Lee, Y.M., and Goodson, H.V. (2004). Molecular evolution of the histone deacetylase family: functional implications of phylogenetic analysis. Journal of Molecular Biology **338**, 17-31.

Heckathron, S.A., Downs, C.A., and Coleman, J.A. (1999). Small heat shock proteins protect electron transport in chloroplasts and mitochondria during stress. American Zoologist **39**, 865–876.

Howell, S.H. (2021). Evolution of the unfolded protein response in plants. Plant, Cell & Environment **44,** 2625-2635.

Hollender, C., and Liu, Z. (2008). Histone deacetylase genes in Arabidopsis development. Journal of Integrative Plant Biology **50,** 875-885.

Ikeda, M., Mitsuda, N., and Ohme-Takagi, M. (2011). Arabidopsis HsfB1 and HsfB2b act as repressors of the expression of heat-inducible Hsfs but positively regulate the acquired thermotolerance. Plant Physiology **157,** 1243-1254.

doi:10.6342/NTU202500611

Klose, R.J., and Zhang, Y. (2007). Regulation of histone methylation by demethylimination and demethylation. Nature Reviews Molecular Cell Biology **8,** 307-318.

Kolmos, E., Chow, B.Y., Pruneda-Paz, J.L., Kay, S.A. (2014). HsfB2b-mediated repression of PRR7 directs abiotic stress responses of the circadian clock. PNAS **111,** 16172-16177.

Kotak, S., Vierling, E., Bäumlein, H., and Koskull-Döring, P.v. (2007). A novel transcriptional cascade regulating expression of heat stress proteins during seed development of Arabidopsis. The Plant Cell **19,** 182-195.

Kumar, S.V., and Wigge, P.A. (2010). H2A.Z-containing nucleosomes mediate the thermosensory response in Arabidopsis. Cell **140,** 136-147.

Larkindale, J., Hall, J.D., Knight, M.R., and Vierling, E. (2005). Heat stress phenotypes of Arabidopsis mutants implicate multiple signaling pathways in the acquisition of thermotolerance. Plant physiology **138,** 882-897.

Lin, K.F., Tsai, M.Y., Lu, C.A., Wu, S.J., and Yeh, C.H. (2018). The roles of Arabidopsis HSFA2, HSFA4a, and HSFA7a in the heat shock response and cytosolic protein response. Botanical Studies **59,** 15.

Liu, C., Lu, F., Cui, X., and Cao, X. (2010). Histone methylation in higher plants. Annual Review of Plant Biology **61,** 395-420.

Liu, H.C., and Charng, Y.Y. (2013). Common and distinct functions of Arabidopsis class A1 and A2 heat shock factors in diverse abiotic stress responses and development. Plant Physiology **163,** 276-290.

Liu, H.C., Liao, H.T., and Charng, Y.Y. (2011). The role of class A1 heat shock factors (HSFA1s) in response to heat and other stresses in Arabidopsis. Plant, Cell & Environment **34,** 738-751.

Liu, X., Yang, S., Zhao, M., Luo, M., Yu, C.W., Chen, C.Y., Tai, R., and Wu, K. (2014). Transcriptional repression by histone deacetylases in plants. Molecular Plant **7,** 764-772.

Lohmann, C., Eggers-Schumacher, G., Wunderlich, M., and Schöffl, F. (2004). Two different heat shock transcription factors regulate immediate early expression of stress genes in Arabidopsis. Molecular Genetics and Genomics **271,** 11-21.

Luger, K., Mäder, A.W., Richmond, R.K., Sargent, D.F., and Richmond, T.J. (1997). Crystal structure of the nucleosome core particle at 2.8 Å resolution. Nature **389**, 251–260.

doi:10.6342/NTU202500611

Luo, M., Tai, R., Yu, C.W., Yang, S., Chen, C.Y., Lin, W.D., Schmidt, W., and Wu, K. (2015). Regulation of flowering time by the histone deacetylase HDA5 in Arabidopsis. Plant Journal **82,** 925-936.

Luo, M., Yu, C.W., Chen, F.F., Zhao, L., Tian, G., Liu, X., Cui, Y., Yang, J.Y., and Wu, K. (2012). Histone deacetylase HDA6 is functionally associated with AS1 in repression of KNOX genes in Arabidopsis. PLoS Genetics **8,** e1003114.

Manghwar, H., and Li, J. (2022). Endoplasmic reticulum stress and unfolded protein response signaling in plants. International Journal of Molecular Sciences **23,** 828

Mittler, R., Finka, A., and Goloubinoff, P. (2012). How do plants feel the heat? Trends in Biochemical Sciences **37,** 118-125.

Nawkar, G.M., Lee, E.S., Shelake, R.M., Park, J.H., Ryu, S.W., Kang, C.H., and Lee, S.Y. (2018). Activation of the transducers of unfolded protein response in plants. Frontiers in Plant Science **9,** 214.

North, B.J., Marshall, B.L., Borra, M.T., Denu J.M., and Verdin, E. (2003). The human Sir2 ortholog, SIRT2, is an NAD+-dependent tubulin deacetylase. Molecular Cell **11,** 437-444.

Nover, L., Bharti, K., Döring, P., Mishra, S.K., Ganguli, A., and Scharf, K.-D. (2001). Arabidopsis and the heat stress transcription factor world: how many heat stress transcription factors do we need? Cell Stress & Chaperones **6,** 177.

Ohama, N., Sato, H., Shinozaki, K., and Yamaguchi-Shinozaki, K. (2017). Transcriptional regulatory network of plant heat stress response. Trends in Plant Science **22,** 53-65.

Pick, T., Jaskiewicz, M., Peterhänsel, C., and Conrath, U. (2012). Heat shock factor HsfB1 primes gene transcription and systemic acquired resistance in Arabidopsis. Plant Physiology **159,** 52-55.

Queitsch, C., Hong, S.W., Vierling, E., and Lindquist, S. (2000). Heat shock protein 101 plays a crucial role in thermotolerance in Arabidopsis. The Plant Cell **12,** 479-492.

Schramm, F., Ganguli, A., Kiehlmann, E., Englich, G., Walch, D., and von Koskull-Doring, P. (2006). The heat stress transcription factor HsfA2 serves as a regulatory amplifier of a subset of genes in the heat stress response in Arabidopsis. Plant Molecular Biology **60,** 759-772.

Scharf, K.D., Siddique, M., and Vierling, E. (2001). The expanding family of small heat shock proteins and their potential for engineering stress tolerance in plants. Plant Physiology **126,** 712-718.

doi:10.6342/NTU202500611

Stroud, H., Do, T., Du, J., Zhong, X., Feng, S., Johnson, L., Patel, D.J., and Jacobsen, S.E. (2014). Non-CG methylation patterns shape the epigenetic landscape in Arabidopsis. Nature Structural & Molecular Biology **21,** 64-72.

Sun, W., Van Montagu, M., and Verbruggen, N. (2002). Small heat shock proteins and stress tolerance in plants. Biochimica et Biophysica Acta **1577,** 1-9.

Tasset, C., Singh Yadav, A., Sureshkumar, S., Singh, R., van der Woude, L., Nekrasov, M., Tremethick, D., van Zanten, M., and Balasubramanian, S. (2018). POWERDRESS-mediated histone deacetylation is essential for thermomorphogenesis in *Arabidopsis thaliana*. PLoS Genetics **14,** e1007280.

Tejedor-Cano, J., Prieto-Dapena, P., Almoguera, C., Carranco, R., Hiratsu, K., Ohme-Takagi, M., and Jordano, J. (2010). Loss of function of the HSFA9 seed longevity program. Plant, Cell & Environment **33,** 1408-1417.

Tilak, P., Kotnik, F., Née, G., Seidel, J., Sindlinger, J., Heinkow, P., Eirich, J., Schwarzer, D., and Finkemeier, I. (2023). Proteome-wide lysine acetylation profiling to investigate the involvement of histone deacetylase HDA5 in the salt stress response of Arabidopsis leaves. Plant Journal **115,** 275-292.

Vierling, E. (1991). The roles of heat shock proteins in plants. Annual Review of Plant Physiology and Plant Molecular Biology **42,** 579-620.

von Koskull-Döring, P., Scharf, K.D., and Nover, L. (2007). The diversity of plant heat stress transcription factors. Trends in Plant Science **12,** 452-457.

Vu, L.D., Gevaert, K., and De Smet, I. (2019). Feeling the heat: searching for plant thermosensors. Trends in Plant Science **24,** 210-219.

Wahid, A., Gelani, S., Ashraf, M., and Foolad, M.R. (2007). Heat tolerance in plants: an overview. Environmental and experimental botany **61,** 199-223.

Wang, W., Ye, R., Xin, Y., Fang, X., Li, C., Shi, H., Zhou, X., and Qi, Y. (2011). An importin β protein negatively regulates MicroRNA activity in Arabidopsis. Plant Cell **23,** 3565-3576.

Wu, C. (1995). Heat Shock Transcription Factors: Structure and Regulation. Annual Review of Cell and Developmental Biology **11,** 441-469.

Wu, F.H., Shen, S.C., Lee, L.Y., Lee, S.H., Chan, M.T., and Lin, C.S. (2009). Tape-Arabidopsis Sandwich - a simpler Arabidopsis protoplast isolation method. Plant Methods **24,** 16.

Yoshida, T., Sakuma, Y., Todaka, D., Maruyama, K., Qin, F., Mizoi, J., Kidokoro, S., Fujita, Y., Shinozaki, K., and Yamaguchi-Shinozaki, K. (2008). Functional analysis of an Arabidopsis heat-shock transcription factor HsfA3 in the

doi:10.6342/NTU202500611

transcriptional cascade downstream of the DREB2A stress-regulatory system. Biochemical and Biophysical Research Communications **368,** 515-521.

Yu, C.W., Liu, X., Luo, M., Chen, C., Lin, X., Tian, G., Lu, Q., Cui, Y., and Wu, K. (2011). HISTONE DEACETYLASE6 interacts with FLOWERING LOCUS D and regulates flowering in Arabidopsis. Plant Physiology **156,** 173-84.

Xu, Y., Li, Q., Yuan, L., Huang, Y., Hung, F.Y., Wu, K., and Yang, S. (2022). MSI1 and HDA6 function interdependently to control flowering time via chromatin modifications. Plant Journal **109,** 831-843.

Zang, D., Wang, J., Zhang, X., Liu, Z., and Wang, Y. (2019). Arabidopsis heat shock transcription factor HSFA7b positively mediates salt stress tolerance by binding to an E-box-like motif to regulate gene expression. Journal of Experimental Botany **70,** 5355-5374.

Zhou, J.J., Cho, J.S., Han, H., Blitz, I.L., Wang, W., and Cho, K.W.Y. (2023). Histone deacetylase 1 maintains lineage integrity through histone acetylome refinement during early embryogenesis. Elife **27,** e79380.

doi:10.6342/NTU202500611

Appendix

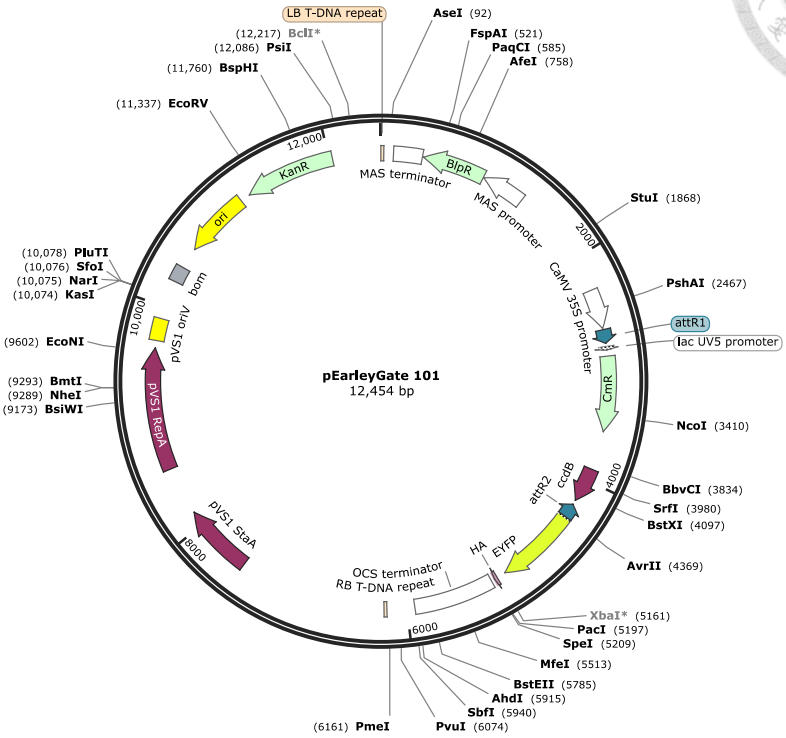

Appendix 1. The map of pEG101 vector for generation of plasmid and overexpression lines.

doi:10.6342/NTU202500611

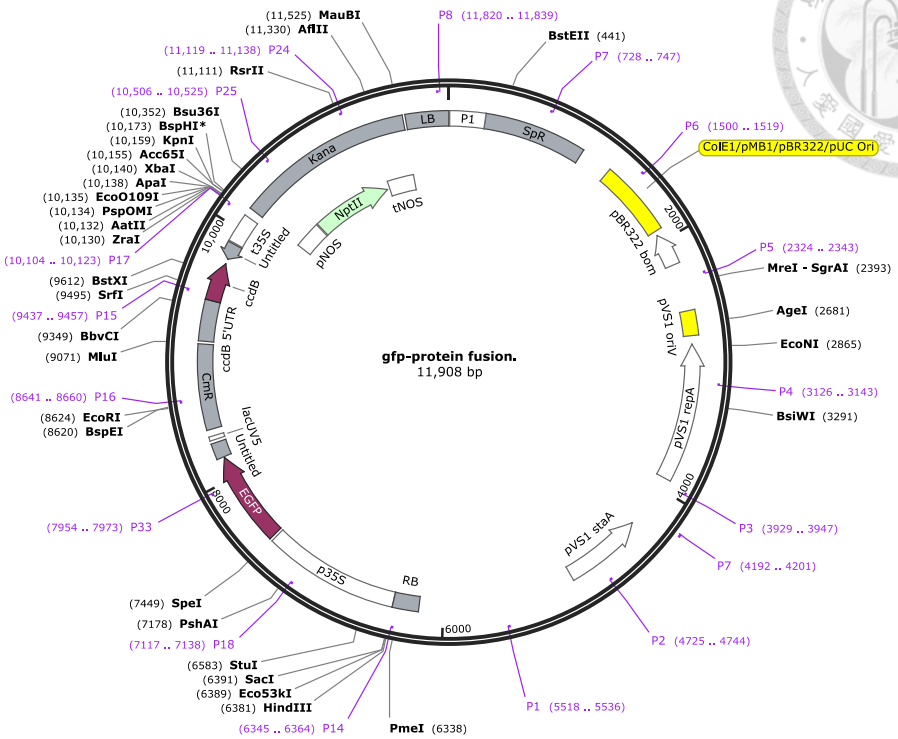

Appendix 2. The map of pK7WGF2 vector for generation of overexpression lines.

doi:10.6342/NTU202500611

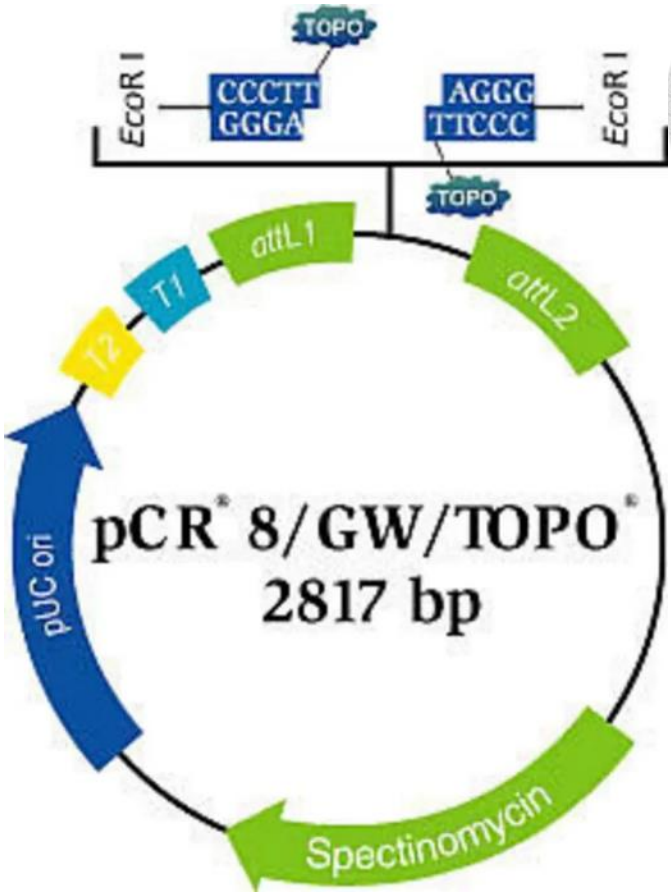

Appendix 3. The map of pCR8/GW/TOPO vector.

doi:10.6342/NTU202500611

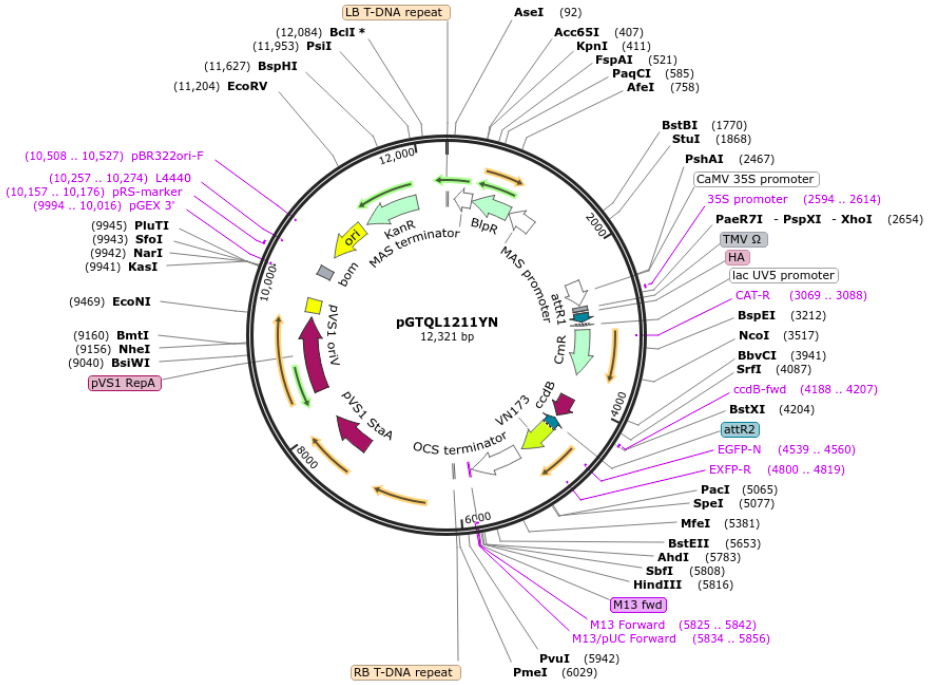

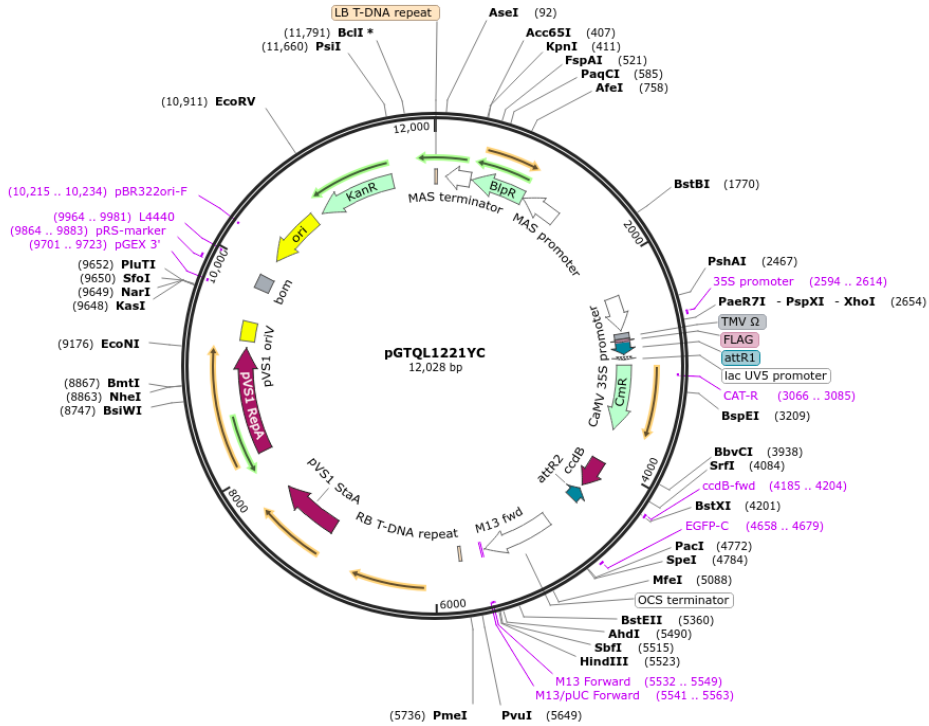

Appendix 4. The map of pGTQL1211YN (pEarleyGate201-YN) and PGTQL1221YC (pEarleyGate202-YC) vectors used for *BiFC* and DLR experiments.

doi:10.6342/NTU202500611

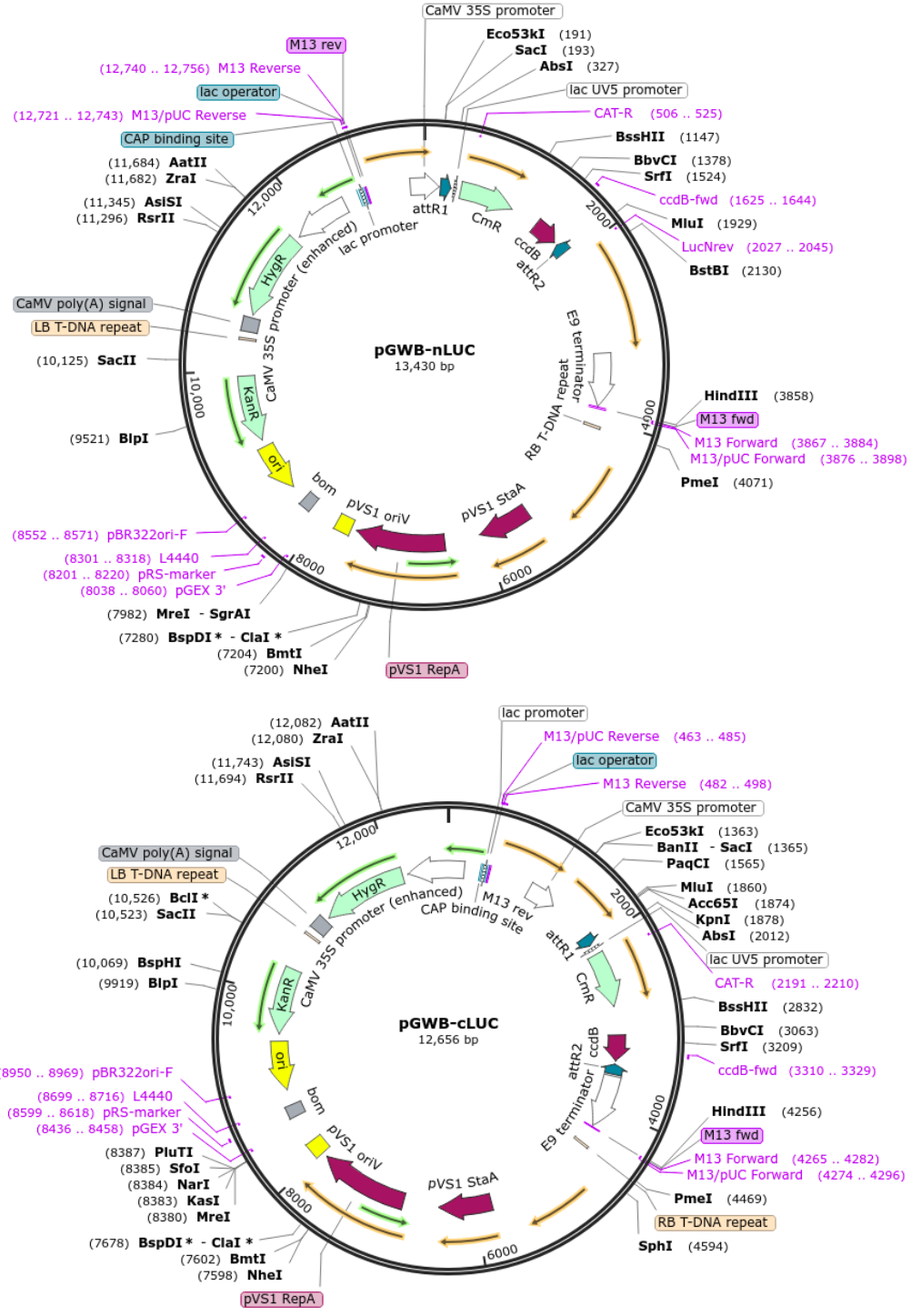

Appendix 5. The map of pGWB-nLUC and pGWB-cLUC vectors used for split-LCI experiments.

doi:10.6342/NTU202500611

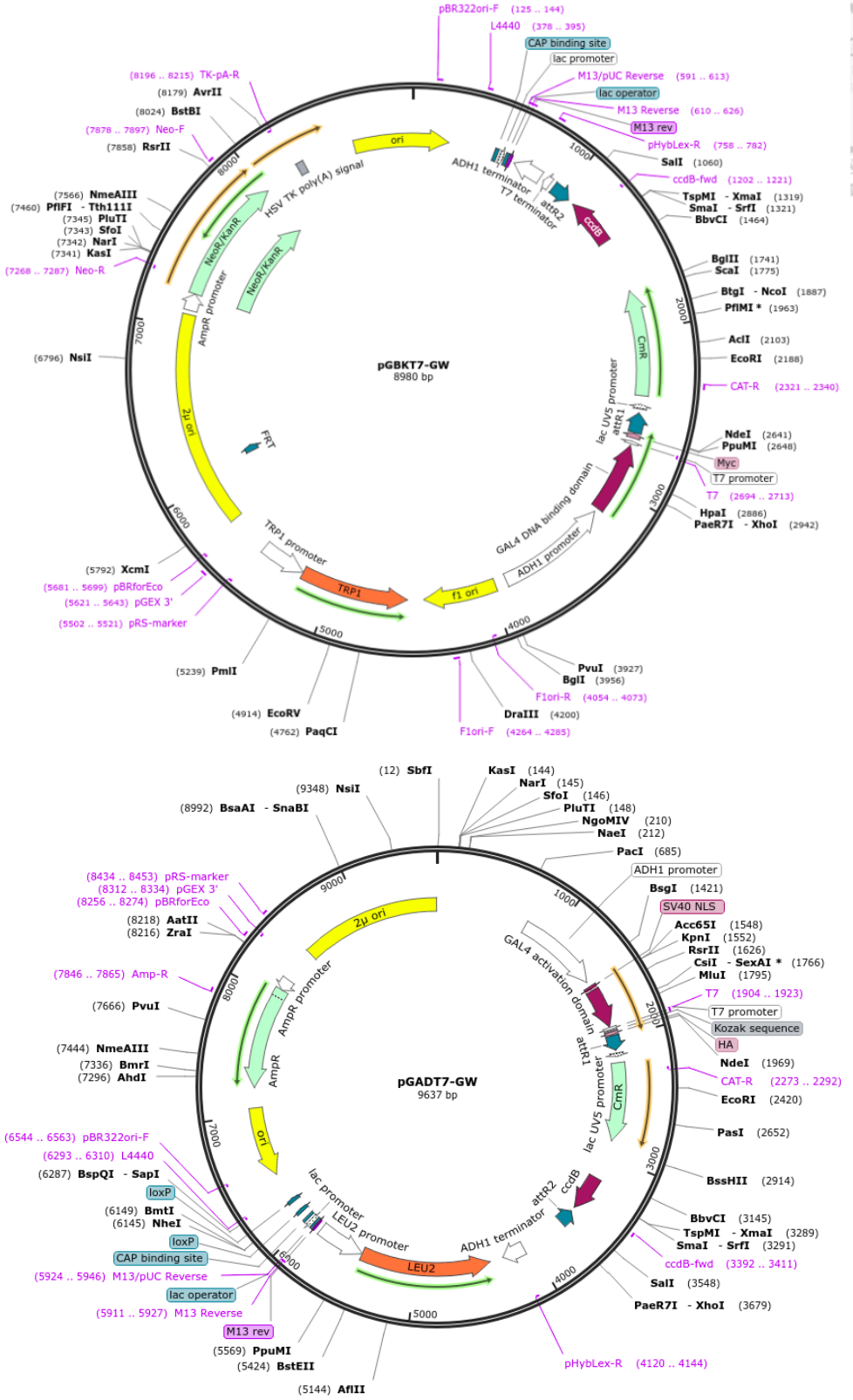

Appendix 6. The map of pGBKD7-GW and pGADT7-GW vectors used for Y2H assay.

doi:10.6342/NTU202500611

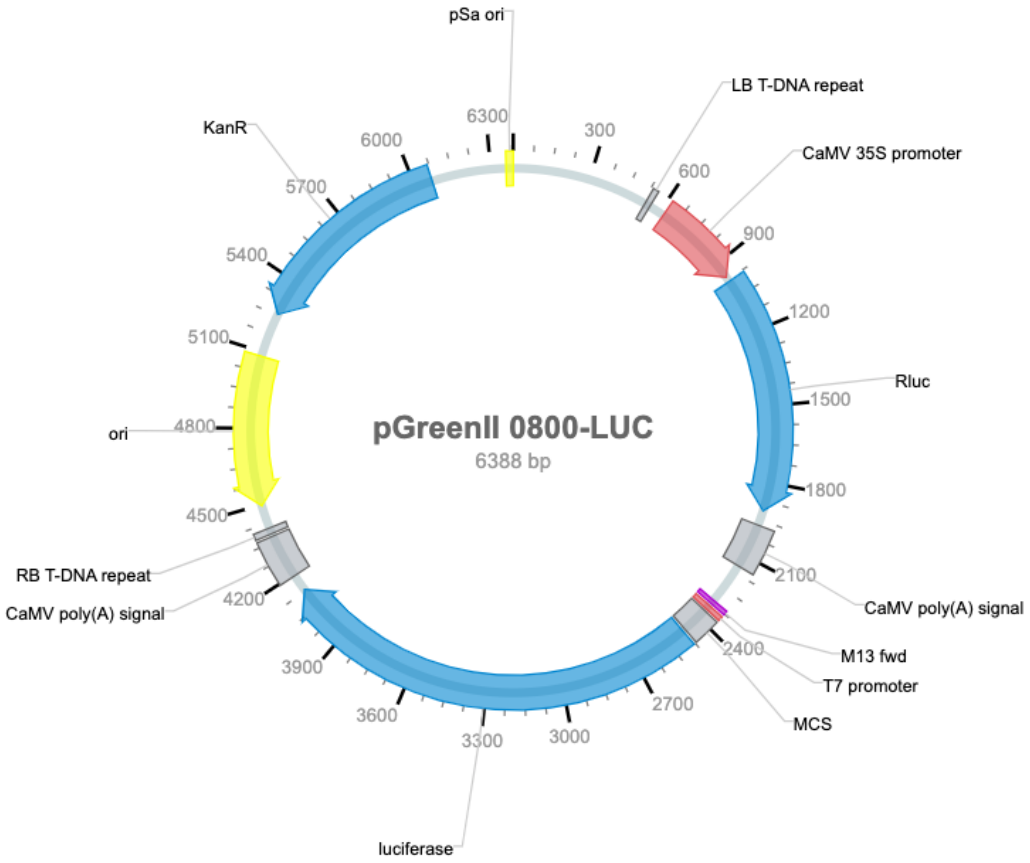

Appendix 7. The map of vector pGreenII 0800-LUC used for promoter of *HSP22* in DLR experiments.

doi:10.6342/NTU202500611